Population size affects adaptation in complex ways: simulations on empirical adaptive landscapes

Vahdati, Ali R ; Wagner, Andreas

Abstract: Do large populations always outcompete smaller ones? Does increasing the mutation rate have a similar effect to increasing the population size, with respect to the adaptation of a population? How important are substitutions in determining the adaptation rate? In this study, we ask how population size and mutation rate interact to affect adaptation on empirical adaptive landscapes. Using such landscapes, we do not need to make many ad hoc assumption about landscape topography, such as about epistatic interactions among mutations or about the distribution of fitness effects. Moreover, we have a better understanding of all the mutations that occur in a population and their effects on the average fitness of the population than we can know in experimental studies. Our results show that the evolutionary dynamics of a population cannot be fully explained by the population mutation rate N Nμ; $even at constant NN\mu, there can be dramatic differences in the adaptation of populations of different sizes. Moreover$

DOI: https://doi.org/10.1007/s11692-017-9440-9

Evolutionary Biology manuscript No.
(will be inserted by the editor)

Population size affects adaptation in complex ways: simulations on empirical adaptive landscapes

Ali R. Vahdati · **Andreas Wagner**

Received: date / Accepted: date

Abstract Do large populations always outcompete smaller ones? Does increasing the mutation rate have a similar effect to increasing the population size, with respect to the adaptation of a population? How important are substitutions in determining the adaptation rate? In this study, we ask how population size and mutation rate interact to affect adaptation on empirical adaptive landscapes. Using such landscapes, we do not need to make many ad hoc assumption about landscape topography, such as about epistatic interactions among mutations or about the distribution of fitness effects. Moreover, we have a better understanding of all the mutations that occur in a population and their effects on the average fitness of the population than we can know in experimental studies. Our results show that the evolutionary dynamics of a population cannot be fully explained by the population mutation rate $N\mu$; even at constant $N\mu$, there can be dramatic differences in the adaptation of populations of different sizes. Moreover, the substitution rate of mutations is not always equivalent to the adaptation rate, because we observed populations adapting to high adaptive peaks without fixing any mutations. Finally, in contrast to some theoretical predictions, even on the most rugged landscapes we study, small population size is never an advantage over larger population size. These result show that complex interactions among multiple factors can affect the evolutionary dynamics of populations, and simple models should be taken with caution.

Keywords Population size · Rate of adaptation · Fitness landscape · Transcription factor binding site

Ali R. Vahdati
Institute of Evolutionary Biology and Environmental Studies, University of Zurich, Zurich, Switzerland
E-mail: ali.rezaee@ieu.uzh.ch
ORCID: 0000-0003-0895-1495

Andreas Wagner
Institute of Evolutionary Biology and Environmental Studies, University of Zurich, Zurich, Switzerland
The Swiss Institute of Bioinformatics, Lausanne, Switzerland
The Santa Fe Institute, Santa Fe, USA
Tel.: +41-44-635-6142
E-mail: andreas.wagner@ieu.uzh.ch

Introduction

How do mutation rate and population size interact on different landscape topographies to affect a population's adaptation? Answering this question can be important for predicting the evolutionary dynamics of different kinds of populations, such as those of pathogens or endangered species. There are many factors affecting the adaptation of organisms, including the presence or absence of genetic recombination; the structure of the fitness landscape (Wright, 1932), e.g. its shape and size; DNA mutation rates; the distribution of fitness effects of mutations; and effective population size (Allen, 2000; McDonald and Linde, 2002; Wilke, 2004; Desai and Fisher, 2007; Desai et al., 2007; Handel and Rozen, 2009; Jain et al., 2011; Lourenço et al., 2013). We focus on two of these factors; namely, effective population size N_e (Charlesworth, 2002; Luikart et al., 2010) and mutation rate μ, to better understand their role in adaptation on empirical adaptive landscapes. Specifically, we would like to know at which mutation rates and levels of landscape ruggedness smaller or larger populations have an evolutionary advantage. Do smaller populations outcompete larger ones when landscape ruggedness increases? What is the role of mutation rate in the adaptation of populations of different sizes?

Population size has a major impact on evolutionary dynamics. Under some circumstances, it is advantageous for a population to be larger. The reason is that natural selection is more effective in removing weakly deleterious mutations and fixing weakly beneficial mutations (Ohta, 1992). Consequently, the beneficial mutations go to fixation more frequently in larger populations, and deleterious mutations go to fixation less frequently (Lanfear et al., 2013; Akashi et al., 2012). Additionally, when the product of population size and mutation rate ($N\mu$) is large enough, an evolving population can cross fitness valleys through a process called stochastic tunneling (Komarova et al., 2003; Iwasa, 2004; Weinreich and Chao, 2005; Weissman et al., 2010; Altland et al., 2011). Specifically, such a population is more likely to produce double mutants that do not experience the deleterious effect of a single mutant, which may allow it to cross a fitness valley (Szendro et al., 2013).

Producing more mutations is not always an advantage. When several beneficial mutations are simultaneously present in an asexual population, they compete with each other for fixation. This slows the time to fixation of a beneficial mutation. This phenomenon is called clonal interference (Gerrish and Lenski, 1998), and it can slow down the rate of adaptive substitutions in a population (Charlesworth and Eyre-Walker, 2006). Producing fewer mutations per generation, smaller populations are less likely to be affected by clonal interference, and they may thus adapt faster (Gerrish and Lenski, 1998; Szendro et al., 2013). Furthermore, genetic drift is stronger in smaller populations. In a rugged landscape, where achieving a higher fitness likely requires passing through fitness valleys, strong genetic drift facilitates valley crossing (Handel and Rozen, 2009; Jain et al., 2011). Moreover, some fitness valleys for large populations become flat for smaller populations, because any fitness difference between two mutations smaller than $1/N$ becomes invisible to selection (Ohta, 1992; Jain et al., 2011; Szendro et al., 2013; Lachapelle et al., 2015).

The many factors affecting evolutionary dynamics often interact in non-intuitive ways to define the evolutionary outcome of a population. Therefore, most previous

theoretical studies include simplifying assumptions to model the role of one or a few of these factors (Desai and Fisher, 2007; Desai et al., 2007; Campos and Wahl, 2010; Lourenço et al., 2013; Lachapelle et al., 2015). Examples include epistatic interactions among mutations (Cordell, 2002; de Visser et al., 2011), and the distribution of fitness effects (Cowperthwaite et al., 2005; Eyre-Walker and Keightley, 2007; Tamuri et al., 2012), which define the ruggedness of a fitness landscape. For example, (Handel and Rozen, 2009) used randomly generated fitness landscapes to study the effect of population size on the evolution of microbes; and (Jain et al., 2011) used a three-locus model with arbitrary fitness values for each genotype to study the advantage of small populations on rugged landscapes. Another example is an assumed distribution of fitness effects with rare beneficial mutations to predict the association between the substitution rate of beneficial mutations and the population size (Lanfear et al., 2013). Whether beneficial mutations are rare depends on the proximity of a population to a fitness peak. Violation of such assumptions can lead to dramatically different evolutionary outcomes (Lanfear et al., 2013). In experimental studies, where realistically complex fitness landscapes are examined (Rozen et al., 2008; Kryazhimskiy et al., 2012), researchers have inevitably limited knowledge about, and control over, underlying evolutionary mechanisms, such as the distribution of fitness effects and the mutational trajectories of a population. This is because such fitness landscapes are usually large, and the possibilities to replicate experiments and to vary parameters are limited.

For these reasons, some studies make contradictory observations about the effect of population size on adaptation. For example, the rate of adaptation, defined as the number of beneficial substitutions, has been predicted to increases with effective population size N_e (Lanfear et al., 2013). However, this prediction only holds when beneficial mutations are rare. The frequency of beneficial mutations, in turn, depends on the location of a population on a fitness landscape and on the topology of the landscape (Lanfear et al., 2013). Thus, some studies have found associations between the N_e and rate of adaptation (Dey et al., 2013), while others have not (Bachtrog, 2008; Karasov et al., 2010; Gayral et al., 2013). Our study tries to fill the gap between theoretical and experimental studies, using a system where we have more knowledge about, and control over, important factors such as population mutation rates, evolutionary trajectories, and the identity of substituted genotypes, than experimental systems. At the same time, we need to make fewer ad hoc assumptions than most previous theoretical studies. One of these assumptions is the distribution of fitness effects. In an empirical landscape, this distribution changes as a population approaches a fitness peak. For example, when a population gets closer to a peak, beneficial mutations become rarer, without the need to make ad hoc assumptions about their frequency.

We consider 957 empirical adaptive landscapes (Aguilar-Rodríguez et al., 2017). Each landscape encompasses the binding affinity of a transcription factor to all of its cognate DNA sequences (i.e., binding sites). These binding affinities are derived from protein binding microarrays in the form of an enrichment score (E-score), which describes the relative binding preference of a transcription factor to all possible DNA sequences of length eight (Berger et al., 2006). The topographies of these landscapes have recently been characterized in rich detail (Aguilar-Rodríguez et al., 2017), which provides an opportunity to study how the topographies of empirical adaptive land-

scapes interact with N and μ to affect the adaptation rate of an evolving population. Transcription factor binding affinity is an important molecular phenotype, because it can affect gene expression. For example, increasing the affinity of an activating transcription factor's binding site will decrease the factor's disassociation rate, thereby increasing the rate of transcription of the downstream gene. If increased expression is selectively advantageous in a given environment (e.g., an antibiotic resistance gene in the presence of an antibiotic), then increased binding affinity may confer increased fitness. The importance of high binding affinity transcription factor binding sites is evidenced by their signature of positive selection in microbes and humans (Mustonen and Lässig, 2005, 2009), as well by their proximity to actively transcribed genes in the embryo of *Drosophila melanogaster* (Li et al., 2008). We therefore use binding affinity as a proxy for fitness.

Using these empirical adaptive landscapes, we do not make any ad hoc assumptions about the distributions of fitness effects, the structure of the landscape, or epistatic interaction among mutations, because such information is implicitly present in the landscapes. We simulate populations with a range of mutation rates μ and population mutation rates $N\mu$, and analyze all mutational trajectories of populations during their evolution. We find that mutation rate μ and population mutation rate $N\mu$ are not always sufficient parameters to predict the adaptation rate of populations on these landscapes. Population diversity and the extent of landscape exploration, rather than the substitution rate of mutations, can affect the adaptation rate.

Methods

Genotype network construction and analysis

Genotype networks were constructed as described in (Payne and Wagner, 2014; Aguilar-Rodríguez et al., 2017). The data for these networks come from in vitro studies that assess the binding affinity of a transcription factor (Latchman, 1997) to all possible DNA sequences of length 8 using protein binding microarrays (Berger et al., 2006; Berger and Bulyk, 2009). The total genotype space consists of 32,896 sequences ($(4^8-4^4)/2+4^4$), where the factor $1/2$ accounts for the merging of sequences with their reverse complement. The number 4^4 accounts for palindromic sequences, which are identical to their reverse complement and therefore cannot be merged (Aguilar-Rodríguez et al., 2017). Reference (Aguilar-Rodríguez et al., 2017) constructed and analyzed 1,137 binding affinity landscapes from 129 different eukaryotic species and 62 DNA binding domain structural classes. For each transcription factor, a protein binding microarray measures the binding affinity of all 8-mers to the factor. The affinity is represented as a rank-based enrichment score (E-score), which is a variant of the Wilcoxon-Mann-Whitney statistic (Berger et al., 2006). This E-score ranges between -0.5 (lowest affinity) to 0.5 (highest affinity). We use the E-score as a proxy for binding affinity, and consider only sequences whose E-score is above 0.35 bound by a transcription factor (Aguilar-Rodríguez et al., 2017). We use this threshold because it has yielded a false discovery rate below 0.001 in 104 mouse transcription factors (Badis et al., 2009a). After identifying a set of sequences that bind each transcription

factor, we constructed genotype networks for each transcription factor. The nodes of the network are DNA sequences. Two nodes are connected by an edge if they differ by a single mutation. The single mutations considered are either point mutations or single nucleotide insertions / deletions. We characterized graph-theoretical properties of these networks using the iGraph library (version 0.7.1) (Csardi and Nepusz, 2006) for Python. We used Gephi (version 0.9.1)(Bastian et al., 2009) for network visualization.

Population evolution model

Each landscape only includes sequences bound by a single transcription factor. However, the total number of sequences of length 8 used in the study (32,896 sequences, either bound to a transcription factor or not bound to any of factors), comprises a bigger network, which we call the network of all possible mutations. For simulations on each landscape, we initialized evolving populations with sequences of low binding affinity, because we wanted to explore the dynamics of populations evolving towards high binding affinity. Specifically, we started each simulation by choosing an arbitrary sequence from the bottom 5% of sequences, according to their E-scores, as the starting sequence of the simulation. Our simulations are limited to the dominant component within each landscape. We initialized a population of N individuals with the same initial sequence. For each set of parameters, we performed 100 simulation replicates, and for each replicate we simulated 1,000 generations of mutation and selection. At each generation, we determined how many mutations each sequence would experience by drawing from a Poisson distribution with a mean equal to the mutation rate μ of the population. If a sequence was to experience one mutation, we chose randomly one of its neighbors in the landscape. If it was to experience two mutations, we first randomly chose one of its neighbors, and then randomly chose one of the neighbors of the neighbor as the mutant, excluding the original sequence (thus prohibiting back mutations), and likewise for any additional mutations. After the mutation step, we assigned a value l to each sequence by assigning a random number defined as its E-score$\pm\Delta$, where Δ is a parameter specific to each landscape, which defines a threshold to call two E-scores different in a protein binding microarray experiment, E-scores of each sequence are measured by two replicates, and Δ is the residual standard error of the linear regression between the E-scores of all bound sequences in the two replicate measurements (Aguilar-Rodríguez et al., 2017). Finally, as the selection step, we randomly sampled exactly N sequences from all the sequences with replacement, where the probability of sampling each sequence was weighted by its value of l. We note that with this selection method, population sizes remain constant every generation.

Neutral neighborhood size calculation

For each landscape, we considered the binding affinity of all neighbors of each of a landscape's sequences. If the binding affinity difference between the sequence and

its neighbor was smaller than $1/N$, the neighbor is part of the neutral neighborhood of the sequence. We report the fraction of neutral neighbors of all sequences in each landscape.

Computing population diversity

We computed two measures of population diversity. The first measure corresponds to the number of unique sequences at the last generation in each simulation. We report its average across 100 simulation replicates. The second measure is the total number of unique sequences that were visited by a population across all generations, averaged over 100 simulation replicates.

Counting the incidence of deleterious, neutral, and beneficial mutations

To calculate the incidence of deleterious, neutral, and beneficial mutations in each population, we tracked every mutation. If the binding affinity difference of sequence and its mutant (whose affinity is given by l defined above, a random number in the range E-score$\pm\Delta$) was more than $1/N$, we considered the mutation non-neutral; it would be beneficial or deleterious depending on whether the binding affinity had increased or decreased, respectively.

Number of substitutions

We considered any sequence different from the ancestral sequence as a sequence that has become fixed if it ever reached a population frequency exceeding 90% (a common practice in simulating populations (Desai and Fisher, 2007; Vatsiou et al., 2016) to limit computational costs). Strictly speaking, fixation means an allele is present in 100% of the population. If a sequence passed the 90% threshold and dropped below this threshold more than once, we considered it as fixed only once.

Results

Structure of binding affinity landscapes

From the 1,137 landscapes studied in (Aguilar-Rodríguez et al., 2017), we simulated the evolution of populations on those 957 landscapes that had at least 100 sequences. We then chose nine of these landscapes for a more detailed analysis. The nine landscapes differ in their ruggedness, as measured by their number of peaks. A peak is defined as a set of sequences whose affinity is larger than that of all their neighboring sequences (Khalid et al., 2016). Table 1 lists the names of these nine transcription factors, their DNA binding domains, the species they belong to, and their number of peaks.

Some landscapes have multiple connected components, i.e. sets of nodes (sequences) that are reachable from one another through a sequence of single step mutations. We call the largest of these components the dominant component and limit our simulations to these dominant components. The single step mutations we consider are either point mutations, or single base pair insertions / deletions (Payne and Wagner, 2014; Aguilar-Rodríguez et al., 2017). The landscapes comprise between 513 and 1,064 sequences, and have between 1 and 13 connected components (Table 1). Figure 1 shows one of the landscapes used in this study, that of the *Arabidopsis thaliana*'s transcriptional repressor AZF2. Each circle represents a sequence and edges connect sequences that differ by a single mutation.

The evolutionary dynamics of a population on an adaptive landscape depends in part on the average fraction of neutral neighbors of its genotypes. When genotypes in a population have larger neutral neighborhoods, the population may be able to explore a larger fraction of the landscape without facing deleterious mutations. Hence, it may more easily discover beneficial mutations and new phenotypes (Ancel and Fontana, 2000). Neutral neighborhood size is a function of effective population size N_e (Hartl and Clark, 1997), which equals consensus population size N in our simulations, because our simulated populations experience no population size fluctuations. We analyzed the size of each neutral neighborhood in different landscapes and with different population sizes. We consider the fitness difference of any two neighboring sequences neutral if it is smaller than $1/N$ (Kimura, 1962; Ohta and Gillespie, 1996). Figure S1 shows the fraction of neutral neighbors among all nodes in a landscape, for all nine different landscapes and different population sizes. As expected, neutral neighborhood size decreases with increasing population size, which makes it more difficult for larger populations to evolve neutrally and cross fitness valleys (Ancel and Fontana, 2000).

We used a variation of the Wright–Fisher model (see Methods) to evolve populations on our landscapes for 1,000 generations of mutation and selection, which favors increases in binding affinity. We performed 100 replications for each simulation. Since we are interested in analyzing the effect of population size N and mutation rate μ on the adaptation of populations, we systematically explored a range of mutation rates ($0.001 \leq \mu \leq 1$) and population mutation rates ($0.01 < N\mu < 10$) with seven population sizes ($10 < N < 640$). We chose a maximum population size of 640 based on the size of the landscapes, so that even in a high mutation regime, only a fraction of the landscape would be occupied by a population.

Landscape ruggedness strongly affects adaptation

We initially determined whether the measurement of ruggedness in these landscapes, namely the number of peaks, affects evolutionary dynamics. To that end, we simulated evolution on all of the 957 landscapes (Aguilar-Rodríguez et al., 2017). We analyzed correlations between the mean final affinity of simulated populations, normalized by the maximum binding affinity in each landscape, and the number of peaks in each landscape, and at different mutation rates. In line with our expectation, populations in more rugged landscapes have lower mean population affinity at the end

of simulations (i.e. generation 1,000) (Table S1). In more rugged landscapes, populations are more likely to get trapped on local optima, and this may be a bigger problem for larger populations, because drift is weaker for them compared to smaller populations. These observations hold for all mutation rates ($\mu = 0.001$ - $\mu = 1$).

We also asked whether the size of (number of sequences in) the global peak of each landscape correlates with the mean final affinity of the populations. We found strong and positive correlations (Table S2): the larger the size of the global peak of a landscape, the higher the mean final affinity of a population. This indicates that larger peaks are easier to find.

Adaptive evolution under varying mutation rate μ

We first investigated how interactions between different mutation rates μ and population sizes N affect population adaptation, using a range of mutation rates between $\mu = 0.001$ and $\mu = 1$.

$\mu = 0.001$

At this low mutation rate, the population mutation rate is $N\mu << 1$ for all population sizes. Larger populations consistently achieve higher mean binding affinity at the end of simulated evolution (Figure 2a). Larger populations have several advantages to help them find adaptive peaks better than smaller populations, even at mutation rates this small. First, since larger populations have a higher population mutation rate $N\mu$, they are slightly more diverse at any generation (Figure 2b). Second, and consequently, larger populations visit more unique sequences (Figure 2c). They are therefore better at exploring the landscape, which gives them more opportunities for identifying adaptive peaks. Third, and in line with the second observation, larger populations fix more mutations, most of which are beneficial (Figure S2). This is because they experience more mutations, and because selection is more effective in larger populations (Jain et al., 2011; Szendro et al., 2013; Lachapelle et al., 2015).

$\mu = 0.01$

At a mutation rate of $\mu = 0.1$, we still find that larger populations have higher mean binding affinity at the end of the evolutionary simulations than smaller populations, although the difference between larger populations is smaller than at $\mu = 0.001$ (Figures 2d and S3). At this mutation rate, populations fall into two evolutionary regimes. Specifically, for four population sizes ($N = 10$, $N = 20$, $N = 40$, and $N = 80$) $N\mu < 1$, and for the other three ($N = 160$, $N = 320$, and $N = 640$) $N\mu > 1$. When there is more than one lineage harboring a beneficial mutation, these lineages compete with each other for fixation, resulting in slower fixation rates of either lineage, a phenomenon called clonal interference (Gerrish and Lenski, 1998). When $N\mu > 1$, populations are polymorphic most of the time, which increases the likelihood of clonal interference (Park and Krug, 2007). We first tested whether we find clonal interference in

these populations, and if it increases with population size. Figure 3 shows the average number of unique mutations that are simultaneously present in the population, and the effect of these mutations, i.e. beneficial, deleterious or neutral, relative to the ancestral sequence of the population. The average number of unique mutations at each generation, and the average number of beneficial unique mutations, increases with population size. Consistent with the existence of clonal interference, we find that the number of beneficial substitutions for most landscapes (all except FBXL19 and kdm2aa) is an increasing function of N when $N\mu < 1$ ($N = 10$, $N = 20$, $N = 40$, and $N = 80$), but a decreasing function of N when $N\mu > 1$ ($N = 160$, $N = 320$, and $N = 640$) (Figure S4). Moreover, despite fixing no more or even fewer beneficial mutations than smaller populations due to increased clonal interference, larger populations reach higher mean final binding affinity. To explain this pattern, we pooled data from all simulations, and asked whether the mean final population binding affinity correlates with two measures of population diversity, i.e. the number of explored sequences during the evolutionary simulation and the amount of standing variation at the final generation. We found strong positive associations between both metrics of diversity and mean final binding affinity (Tables S4 and S5). Note that larger populations are both more diverse in the last generation (Figure 2e) and explore more sequences during evolution (Figure 2f). These observations suggest that, unsurprisingly, larger populations have more standing variation, which increases the prevalence of beneficial mutations (Figure S5), which in turn is strongly associated with increased mean population binding affinity (Table S6). In sum, the mean final binding affinity of evolving populations is not completely determined by the number of beneficial substitutions, but also by the population diversity.

$\mu = 0.1$

At a mutation rate of $\mu = 0.1$, the population mutation rate is $N\mu > 1$ for all populations, and clonal interference is prevalent in all populations, but becomes stronger in larger populations (Figure S6). The largest populations ($N = 160$, $N = 320$, and $N = 640$), therefore, have nearly no substitutions (Figure S7). Still, they arrive at a higher mean binding affinity than smaller populations (Figure 4a). The largest populations in some landscapes (FBXL19, NCU00445, and TIFY2B), however, do not differ in their mean final binding affinity.

Population diversity can help explain how larger populations reach higher mean binding affinity levels, despite fixing nearly no mutations. Larger populations explore more sequences than smaller populations, and the difference in this exploration ability between larger and smaller populations is greater at $\mu = 0.1$ (Figure 4c). Similarly, the difference between the fraction of beneficial mutations among all mutations that occur in larger populations and in smaller populations is greater at $\mu = 0.1$ (compare Figures S5 and S8).

$\mu = 1$

At this large mutation rate, where on average every sequence mutates in every generation ($N\mu >> 1$), we do not find striking differences between the mean final binding

affinity at different population sizes (Figure 4d). Only the two smallest populations ($N = 10$ and $N = 20$) have a slightly lower mean binding affinity than larger populations. More pronounced, however, is a drop in mean final binding affinity of all population sizes compared with $\mu = 0.1$ (compare Figure 4a with 4d). This is because of the high fraction of mutant individuals that are created generation. When a population finds and moves to a sequence with a high binding affinity, it will not stay there, because at the next generation, most individuals mutate away from it. Therefore, the mean affinity of populations fluctuates around lower values and the highest possible mean affinities cannot be attained.

Adaptive evolution under varying population mutation rates $N\mu$

Another important quantity in population genetics is the population mutation rate $N\mu$. In the following sections, we will analyze the effect of $N\mu$ on adaptive evolution to find out whether it alone can explain the difference in adaptation between populations of different sizes.

$N\mu = 0.01$ *and* $N\mu = 0.1$

At these low population mutation rates, populations of all sizes reach similar mean final binding affinity levels (Figures 5a and 5b). Likewise, the extent of sequence exploration (Figures S9 S10) and population diversity in the last generation (Figures S11 and S12) is similar among populations of all different sizes. This suggests that $N\mu$ may be adequate to explain evolutionary dynamics when $N\mu$ is not too large.

$N\mu = 1$ *and* $N\mu = 10$

At the moderate population mutation rate of $N\mu = 1$, we find that the smallest populations (i.e. $N = 10$, $N = 20$, and $N = 40$) are not reaching the same mean final binding affinity as larger populations (Figure 5c). At the high population mutation rate $N\mu = 10$, this dependency of final fitness on population size is even stronger (Figure 5d). In addition, there is a negative association between sequence exploration and population size (Figures S13 and S14). This is likely due to larger neutral neighborhood that is characteristic of smaller populations (Figure S1). Larger neutral neighborhoods mean that more neutral mutations are available to smaller populations (Figures S15 and S16), which thus face fewer limitations exploring novel sequences. Such larger neutral neighborhoods also result in more neutral substitutions in smaller populations (Figures S17 and S18). Larger populations experience (Figure S19) and fix more beneficial mutations than smaller populations (Figure S20) at $N\mu = 1$. At $N\mu = 10$, however, we observe a peak in the maximum fraction of beneficial mutations that the populations experience at intermediate population sizes (Figure S21). All populations at $N\mu = 10$ fix fewer mutations than at $N\mu = 1$, but larger populations fix more beneficial mutations (Figure S22). Two factors can explain the difference in mean final binding affinity between smaller and larger populations at constant and large population mutation rates. First, selection is more effective at fixing beneficial

mutation in larger population. Second, and more importantly, the constant high population mutation rate has a negative effect on the ability to reach high mean affinity for smaller populations, but not for larger populations. A value of $N\mu = 10$ means that an average of ten new mutations are introduced into a population each generation. For a population of size 10, this means that at every generation all individuals are mutated. In a population of size 20, half of all individuals are mutated, but in a population of size 640, only a fraction of 0.016 of individuals are mutated. The high number of mutations overwhelms selection in small populations, making it difficult for small populations to follow a gradual affinity–increasing path.

Discussion

To understand the rate and limitations of organismal adaptation is a central to evolutionary biology (Lynch and Lande, 1998; Allen, 2000; Franklin and Frankham, 1998; Stockwell et al., 2003; de Visser and Rozen, 2005; Barrick et al., 2009; Wiser et al., 2013). Efforts to increase our understanding in this area can be divided into two major classes based on their methodology. The first uses theoretical approaches (Desai and Fisher, 2007; Desai et al., 2007; Campos and Wahl, 2010; Lourenço et al., 2013). Due to the complex interactions between different factors, such as mutation rate, changes in effective population size, recombination rate, etc., these approaches usually make many simplifying assumptions, which may not always hold in biological populations. The second class uses experiments (Lenski et al., 1991; Lenski and Travisano, 1994; Elena and Lenski, 2003; Lachapelle et al., 2015), which can examine a biological system in its full complexity. However, they provide limited knowledge about the important evolutionary mechanisms, such as the effects of mutations on a population's trajectories, and a fitness landscape's structure. In addition, the ability to replicate experiments and to test different parameters in them is limited.

Here, we used a system that bridges these two approaches. We simulated evolving populations on 957 empirical adaptive landscapes of transcription factor binding sites, and analyzed the evolutionary dynamics on nine such landscapes (Aguilar-Rodríguez et al., 2017). We considered the binding affinity between transcription factor and DNA sequences as a proxy for fitness. With such landscapes, we did not have to make ad hoc assumptions about epistatic interactions between mutations, about the distribution of fitness effects, or about landscapes structures. Additionally, we could study the effects of all mutations, and could examine the and mutational trajectories of populations in detail. We found complex interactions between mutation rate and population size, as described below.

Firstly, we found that at any mutation rate, larger populations are better at increasing their mean final affinity (Figure 4a). This is intriguing, because at high $N\mu$, due to increased clonal interference, large populations hardly fix any mutations (Figure S7); and because the substitution rate, especially that of beneficial mutations, is commonly treated as a measure of adaptation rate (Park and Krug, 2007; Campos and Wahl, 2009, 2010; Gossmann et al., 2012; Lanfear et al., 2013; Pokalyuk et al., 2013; Wong and Seguin, 2015). The likely reason that substitution rate does not always determine adaptation is this: Larger populations are more diverse at any given

time, and thus explore more sequences in a landscape than smaller populations, which means that they can find beneficial mutations more easily. The presence of multiple beneficial mutations in a population helps the population increase its mean binding affinity, even if no mutation is fixed. This is akin to a soft selective sweep (Losos et al., 2013, p. 472), where multiple beneficial mutations occur and increase their frequency in a population without any of them being fixed (Hermisson and Pennings, 2005; Pennings and Hermisson, 2006).

Second, we found that even at constant $N\mu$ and for different population sizes, when $N\mu$ is large enough, smaller populations fail to find adaptive peaks as effectively as larger populations (Figure 5d). The reason is that at constant population mutation rates, smaller populations have a higher mutation rate per genotype than the larger populations. This higher mutation rate overwhelms the small populations and prevents them from following an affinity-increasing path.

Third, we found that sequence exploration and population diversity almost always depend on population size N, even when population mutation rates $N\mu$ are constant (Figure S14). The only exception is when the population mutation rate $N\mu$ is so low that all populations explore equally few sequences (Figure S9).

In sum, we found that smaller populations have no adaptive advantage over larger ones, even when $N\mu$ is constant for populations at different sizes, because smaller populations do not have higher mean final affinity at the end of our simulations. This observation holds regardless of landscape ruggedness, because the landscapes we studied varied in their ruggedness (Table 1). In theory, smaller populations could have several advantages on rugged landscapes (Rozen et al., 2008), such as higher chances of escaping local optima, and larger neutral neighborhoods, which could help them explore more sequences, some of which could boost their adaptation. However, these advantages did not lead to better adaptation on the landscapes studied here.

Our study has limitations, which can be alleviated in future work. Firstly, we studied clonal populations with no recombination. It would be interesting to see how populations adapt on our landscapes in the presence of recombination, because recombination can dramatically affect evolutionary dynamics (Muller, 1932; Evans, 1986; Ochman et al., 2000; Zhang et al., 2002; Otto and Gerstein, 2006; Cooper, 2007). Moreover, we used the number of peaks as a measure of landscape ruggedness. It would be interesting to compare the topology of these landscapes with random landscapes used in previous studies, where smaller populations do have an adaptive advantage over larger ones. For example, (Handel and Rozen, 2009) constructed random landscapes with different numbers of peaks (ruggedness). They simulated populations evolving on the landscapes, and observed that on landscapes with a minimum amount of ruggedness, smaller populations can reach a higher final fitness, because they do not get trapped on local peaks. The conditions that provide an advantage to smaller populations in such theoretical studies may also exist in other empirical landscapes. A third limitation is that we have assumed a one-to-one relationship between binding affinity to a transcription factor and its fitness. However, the exact relationship between affinity and fitness is not known. Changes in this relationship could result in major changes in the structure of landscape (its ruggedness, number of peaks, and accessibility), and thus affect the results we have obtained.

In sum, our results show that in empirical adaptive landscapes, there are complex interdependencies between population size and mutation rate that affect evolutionary dynamics, especially at high $N\mu$, suggesting that conclusions from simplified models should be taken with caution.

Competing interests

The authors declare that they have no competing interests.

Ethical standards

Not applicable.

Acknowledgements AW acknowledges support by ERC Advanced Grant 739874, by Swiss National Science Foundation grant 31003A_172887, as well as by the University Priority Research Program in Evolutionary Biology at the University of Zurich. We are indebted to Joshua L. Payne for data analysis and helps and suggestions on the paper.

References

J. Aguilar-Rodríguez, J. L. Payne, and A. Wagner. A thousand empirical adaptive landscapes and their navigability. *Nature Ecology & Evolution*, 1(2):0045, 2017. ISSN 2397-334X. doi: 10.1038/s41559-016-0045.

H. Akashi, N. Osada, and T. Ohta. Weak selection and protein evolution. *Genetics*, 192(1):15–31, sep 2012. ISSN 0016-6731. doi: 10.1534/genetics.112.140178.

A. Allen. The rate of adaptation in asexuals. *Genetics*, 155(2):961–968, 2000. ISSN 00166731.

A. Altland, A. Fischer, J. Krug, and I. G. Szendro. Rare events in population genetics: stochastic tunneling in a two-locus model with recombination. *Physical Review Letters*, 106(8):088101, feb 2011. ISSN 1079-7114. doi: 10.1103/PhysRevLett.106.088101.

L. W. Ancel and W. Fontana. Plasticity, evolvability, and modularity in RNA. *The Journal of Experimental Zoology*, 288(3):242–83, oct 2000. ISSN 0022-104X.

D. Bachtrog. Similar rates of protein adaptation in *Drosophila miranda* and *D. melanogaster*, two species with different current effective population sizes. *BMC Evolutionary Biology*, 8(1):334, 2008. ISSN 1471-2148. doi: 10.1186/1471-2148-8-334.

G. Badis, M. F. Berger, A. A. Philippakis, S. Talukder, A. R. Gehrke, S. A. Jaeger, E. T. Chan, G. Metzler, A. Vedenko, X. Chen, H. Kuznetsov, C.-F. Wang, D. Coburn, D. E. Newburger, Q. Morris, T. R. Hughes, and M. L. Bulyk. Diversity and complexity in DNA recognition by transcription factors. *Science*, 324(5935):1720–3, jun 2009a. ISSN 1095-9203. doi: 10.1126/science.1162327.

G. Badis, M. F. Berger, A. A. Philippakis, S. Talukder, A. R. Gehrke, S. A. Jaeger, E. T. Chan, G. Metzler, A. Vedenko, X. Chen, H. Kuznetsov, C.-F. Wang,

D. Coburn, D. E. Newburger, Q. Morris, T. R. Hughes, and M. L. Bulyk. Diversity and complexity in DNA recognition by transcription factors. *Science*, 324(5935): 1720–1723, jun 2009b. ISSN 0036-8075. doi: 10.1126/science.1162327.

J. E. Barrick, D. S. Yu, S. H. Yoon, H. Jeong, T. K. Oh, D. Schneider, R. E. Lenski, and J. F. Kim. Genome evolution and adaptation in a long-term experiment with *Escherichia coli*. *Nature*, 461(7268):1243–1247, oct 2009. ISSN 1476-4687. doi: 10.1038/nature08480.

M. Bastian, S. Heymann, and M. Jacomy. Gephi: an open source software for exploring and manipulating networks. *International AAAI Conference on Weblogs and Social Media*, oct 2009.

M. F. Berger and M. L. Bulyk. Universal protein-binding microarrays for the comprehensive characterization of the DNA-binding specificities of transcription factors. *Nature Protocols*, 4(3):393–411, mar 2009. ISSN 1754-2189. doi: 10.1038/nprot.2008.195.

M. F. Berger, A. A. Philippakis, A. M. Qureshi, F. S. He, P. W. Estep, and M. L. Bulyk. Compact, universal DNA microarrays to comprehensively determine transcription-factor binding site specificities. *Nature Biotechnology*, 24(11):1429–1435, nov 2006. ISSN 1087-0156. doi: 10.1038/nbt1246.

P. R. A. Campos and L. M. Wahl. The effects of population bottlenecks on clonal interference, and the adaptation effective population size. *Evolution*, 63(4):950–958, apr 2009. ISSN 00143820. doi: 10.1111/j.1558-5646.2008.00595.x.

P. R. A. Campos and L. M. Wahl. The adaptation rate of asexuals: deleterious mutations, clonal interference and population bottlenecks. *Evolution*, 64(7):1973–1983, apr 2010. ISSN 00143820. doi: 10.1111/j.1558-5646.2010.00981.x.

B. Charlesworth. Effective population size. *Current Biology*, 12(21):R716–R717, oct 2002. ISSN 09609822. doi: 10.1016/S0960-9822(02)01244-7.

J. Charlesworth and A. Eyre-Walker. The rate of adaptive evolution in enteric bacteria. *Molecular Biology and Evolution*, 23(7):1348–56, jul 2006. ISSN 0737-4038. doi: 10.1093/molbev/msk025.

T. F. Cooper. Recombination speeds adaptation by reducing competition between beneficial mutations in populations of *Escherichia coli*. *PLoS Biology*, 5(9):e225, sep 2007. ISSN 1545-7885. doi: 10.1371/journal.pbio.0050225.

H. J. Cordell. Epistasis: what it means, what it doesn't mean, and statistical methods to detect it in humans. *Human Molecular Genetics*, 11(20):2463–2468, oct 2002. ISSN 14602083. doi: 10.1093/hmg/11.20.2463.

M. C. Cowperthwaite, J. J. Bull, and L. A. Meyers. Distributions of beneficial fitness effects in RNA. *Genetics*, 170(4):1449–57, aug 2005. ISSN 0016-6731. doi: 10.1534/genetics.104.039248.

G. Csardi and T. Nepusz. The igraph software package for complex network research. *InterJournal*, Complex Systems:1695, 2006.

J. A. G. M. de Visser and D. E. Rozen. Limits to adaptation in asexual populations. *Journal of Evolutionary Biology*, 18(4):779–88, jul 2005. ISSN 1010-061X. doi: 10.1111/j.1420-9101.2005.00879.x.

J. A. G. M. de Visser, T. F. Cooper, and S. F. Elena. The causes of epistasis. *Proceedings of the Royal Society B Biological Sciences*, 278(1725):3617–24, dec 2011. ISSN 1471-2954. doi: 10.1098/rspb.2011.1537.

M. M. Desai and D. S. Fisher. Beneficial mutation-selection balance and the effect of linkage on positive selection. *Genetics*, 176(3):1759–1798, 2007. ISSN 00166731. doi: 10.1534/genetics.106.067678.

M. M. Desai, D. S. Fisher, and A. W. Murray. The speed of evolution and maintenance of variation in asexual populations. *Current Biology*, 17(5):385–394, mar 2007. ISSN 09609822. doi: 10.1016/j.cub.2007.01.072.

A. Dey, C. K. W. Chan, C. G. Thomas, and A. D. Cutter. Molecular hyperdiversity defines populations of the nematode Caenorhabditis brenneri. *Proceedings of the National Academy of Sciences*, 110(27):11056–11060, jul 2013. ISSN 0027-8424. doi: 10.1073/pnas.1303057110.

S. F. Elena and R. E. Lenski. Evolution experiments with microorganisms: the dynamics and genetic bases of adaptation. *Nature Reviews. Genetics*, 4(6):457–469, jun 2003. ISSN 14710056. doi: 10.1038/nrg1088.

R. Evans. Niche expansion in bacteria: can infectious gene exchange affect the rate of evolution? *Genetics*, 113(3):775–95, jul 1986. ISSN 0016-6731.

A. Eyre-Walker and P. D. Keightley. The distribution of fitness effects of new mutations. *Nature Reviews. Genetics*, 8(8):610–8, aug 2007. ISSN 1471-0056. doi: 10.1038/nrg2146.

I. R. Franklin and R. Frankham. How large must populations be to retain evolutionary potential? *Animal Conservation*, 1(1):69–70, feb 1998. ISSN 1367-9430. doi: 10.1111/j.1469-1795.1998.tb00228.x.

P. Gayral, J. Melo-Ferreira, S. Glémin, N. Bierne, M. Carneiro, B. Nabholz, J. M. Lourenco, P. C. Alves, M. Ballenghien, N. Faivre, K. Belkhir, V. Cahais, E. Loire, A. Bernard, and N. Galtier. Reference-free population genomics from next-generation transcriptome data and the vertebrate–invertebrate gap. *PLoS Genetics*, 9(4):e1003457, apr 2013. ISSN 1553-7404. doi: 10.1371/journal.pgen.1003457.

P. J. Gerrish and R. E. Lenski. The fate of competing beneficial mutations in an asexual population. *Genetica*, 102-103(1-6):127–44, 1998. ISSN 0016-6707. doi: 10.1023/A:1017067816551.

T. I. Gossmann, P. D. Keightley, and A. Eyre-Walker. The effect of variation in the effective population size on the rate of adaptive molecular evolution in eukaryotes. *Genome Biology and Evolution*, 4(5):658–667, 2012. ISSN 17596653. doi: 10.1093/gbe/evs027.

A. Handel and D. E. Rozen. The impact of population size on the evolution of asexual microbes on smooth versus rugged fitness landscapes. *BMC Evolutionary Biology*, 9:236, 2009. ISSN 1471-2148. doi: 10.1186/1471-2148-9-236.

D. L. Hartl and A. G. Clark. *Principles of population genetics*. Sinauer Associates, Inc., Sunderland, Massachusetts, third edition, 1997. ISBN 0-87893-306-9.

J. Hermisson and P. S. Pennings. Soft sweeps: molecular population genetics of adaptation from standing genetic variation. *Genetics*, 169(4):2335–52, apr 2005. ISSN 0016-6731. doi: 10.1534/genetics.104.036947.

Y. Iwasa. Stochastic tunnels in evolutionary dynamics. *Genetics*, 166(3):1571–1579, mar 2004. ISSN 0016-6731. doi: 10.1534/genetics.166.3.1571.

K. Jain, J. Krug, and S.-C. C. Park. Evolutionary advantage of small populations on complex fitness landscapes. *Evolution*, 65(7):1945–1955, jul 2011. ISSN 00143820. doi: 10.1111/j.1558-5646.2011.01280.x.

T. Karasov, P. W. Messer, and D. A. Petrov. Evidence that adaptation in Drosophila is not limited by mutation at single sites. *PLoS Genetics*, 6(6):e1000924, jun 2010. ISSN 1553-7404. doi: 10.1371/journal.pgen.1000924.

F. Khalid, J. Aguilar-Rodríguez, A. Wagner, and J. L. Payne. Genonets server-a web server for the construction, analysis and visualization of genotype networks. *Nucleic Acids Research*, 44(W1):gkw313, jul 2016. ISSN 1362-4962. doi: 10.1093/nar/gkw313.

M. Kimura. On the probability of fixation of mutant genes in a population. *Genetics*, 47(6):713–719, 1962.

N. L. Komarova, A. Sengupta, and M. A. Nowak. Mutation-selection networks of cancer initiation: tumor suppressor genes and chromosomal instability. *Journal of Theoretical Biology*, 223(4):433–450, aug 2003. ISSN 00225193. doi: 10.1016/S0022-5193(03)00120-6.

S. Kryazhimskiy, D. P. Rice, and M. M. Desai. Population subdivision and adaptation in asexual populations of *Saccharomyces cerevisiae*. *Evolution*, 66(6):1931–1941, 2012. ISSN 00143820. doi: 10.1111/j.1558-5646.2011.01569.x.

J. Lachapelle, J. Reid, and N. Colegrave. Repeatability of adaptation in experimental populations of different sizes. *Proceedings of the Royal Society B: Biological Sciences*, 282(1805):20143033–20143033, mar 2015. ISSN 0962-8452. doi: 10.1098/rspb.2014.3033.

R. Lanfear, H. Kokko, and A. Eyre-Walker. Population size and the rate of evolution. *Trends in Ecology & Evolution*, pages 1–9, oct 2013. ISSN 01695347. doi: 10.1016/j.tree.2013.09.009.

D. S. Latchman. Transcription factors: An overview. *The International Journal of Biochemistry & Cell Biology*, 29(12):1305–1312, dec 1997. ISSN 13572725. doi: 10.1016/S1357-2725(97)00085-X.

R. E. Lenski and M. Travisano. Dynamics of adaptation and diversification: a 10,000-generation experiment with bacterial populations. *Proceedings of the National Academy of Sciences of the United States of America*, 91(15):6808–6814, 1994. ISSN 0027-8424. doi: 10.1073/pnas.91.15.6808.

R. E. Lenski, M. R. Rose, and S. C. Simpson. Long-term experimental evolution in *Escherichia coli*. I. Adaptation and divergence during 2,000 generations. *American Naturalist*, 138(6):1315–1341, 1991.

X.-y. Li, S. MacArthur, R. Bourgon, D. Nix, D. A. Pollard, V. N. Iyer, A. Hechmer, L. Simirenko, M. Stapleton, C. L. Luengo Hendriks, H. C. Chu, N. Ogawa, W. Inwood, V. Sementchenko, A. Beaton, R. Weiszmann, S. E. Celniker, D. W. Knowles, T. Gingeras, T. P. Speed, M. B. Eisen, and M. D. Biggin. Transcription factors bind thousands of active and inactive regions in the Drosophila blastoderm. *PLoS Biology*, 6(2):e27, feb 2008. ISSN 1545-7885. doi: 10.1371/journal.pbio.0060027.

J. B. Losos, D. A. Baum, D. J. Futuyma, H. E. Hoekstra, R. E. Lenski, A. J. Moore, C. L. Peichel, D. Schluter, and M. C. Whitlock. *The Princeton guide to evolution*. Princeton University Press, Princeton, 2013. ISBN 0691149771.

J. M. Lourenço, S. Glémin, and N. Galtier. The rate of molecular adaptation in a changing environment. *Molecular Biology and Evolution*, 30(6):1292–1301, jun 2013. ISSN 07374038. doi: 10.1093/molbev/mst026.

G. Luikart, N. Ryman, D. A. Tallmon, M. K. Schwartz, and F. W. Allendorf. Estimation of census and effective population sizes: the increasing usefulness of DNA-based approaches. *Conservation Genetics*, 11(2):355–373, apr 2010. ISSN 1566-0621. doi: 10.1007/s10592-010-0050-7.

M. Lynch and R. Lande. The critical effective size for a genetically secure population. *Animal Conservation*, 01(01):S136794309822110X, feb 1998. ISSN 13679430. doi: 10.1017/S136794309822110X.

B. a. McDonald and C. Linde. Pathogen population genetics, evolutionary potential, and durable resistance. *Annual Review of Phytopathology*, 40:349–79, jan 2002. ISSN 0066-4286. doi: 10.1146/annurev.phyto.40.120501.101443.

H. J. Muller. Some genetic aspects of sex. *The American Naturalist*, 66(703):118–138, mar 1932. ISSN 0003-0147. doi: 10.1086/280418.

V. Mustonen and M. Lässig. Evolutionary population genetics of promoters: predicting binding sites and functional phylogenies. *Proceedings of the National Academy of Sciences of the United States of America*, 102(44):15936–15941, 2005. ISSN 0027-8424. doi: 10.1073/pnas.0505537102.

V. Mustonen and M. Lässig. From fitness landscapes to seascapes: non-equilibrium dynamics of selection and adaptation. *Trends in Genetics*, 25(3):111–9, mar 2009. ISSN 0168-9525. doi: 10.1016/j.tig.2009.01.002.

H. Ochman, J. G. Lawrence, and E. A. Groisman. Lateral gene transfer and the nature of bacterial innovation. *Nature*, 405(6784):299–304, may 2000. ISSN 0028-0836. doi: 10.1038/35012500.

T. Ohta. The nearly neutral theory of molecular evolution. *Annual Review of Ecology and Systematics*, 23(1992):263–286, 1992. ISSN 00664162. doi: 10.2307/2097289.

T. Ohta and J. Gillespie. Development of neutral and nearly neutral theories. *Theoretical Population Biology*, 49(2):128–42, 1996. ISSN 1096-0325. doi: 10.1006/tpbi.1996.0007.

S. P. Otto and A. C. Gerstein. Why have sex? The population genetics of sex and recombination. *Biochemical Society Transactions*, 34(Pt 4):519–22, aug 2006. ISSN 0300-5127. doi: 10.1042/BST0340519.

S.-C. Park and J. Krug. Clonal interference in large populations. *Proceedings of the National Academy of Sciences of the United States of America*, 104(46):18135–40, nov 2007. ISSN 1091-6490. doi: 10.1073/pnas.0705778104.

J. L. Payne and A. Wagner. The robustness and evolvability of transcription factor binding sites. *Science*, 343(6173):875–877, feb 2014. ISSN 0036-8075. doi: 10.1126/science.1249046.

P. S. Pennings and J. Hermisson. Soft sweeps II–molecular population genetics of adaptation from recurrent mutation or migration. *Molecular Biology and Evolution*, 23(5):1076–84, may 2006. ISSN 0737-4038. doi: 10.1093/molbev/msj117.

C. Pokalyuk, L. A. Mathew, D. Metzler, and P. Pfaffelhuber. Competing islands limit the rate of adaptation in structured populations. *Theoretical Population Biology*, 90:1–11, 2013. ISSN 00405809. doi: 10.1016/j.tpb.2013.08.001.

D. E. Rozen, M. G. J. L. Habets, A. Handel, and J. A. G. M. de Visser. Heterogeneous adaptive trajectories of small populations on complex fitness landscapes. *PloS One*, 3(3):e1715, jan 2008. ISSN 1932-6203. doi: 10.1371/journal.pone.0001715.

C. A. Stockwell, A. P. Hendry, and M. T. Kinnison. Contemporary evolution meets conservation biology. *Trends in Ecology & Evolution*, 18(2):94–101, feb 2003. ISSN 01695347. doi: 10.1016/S0169-5347(02)00044-7.

I. G. Szendro, J. Franke, J. A. G. M. de Visser, and J. Krug. Predictability of evolution depends nonmonotonically on population size. *Proceedings of the National Academy of Sciences*, 110(2):571–576, jan 2013. ISSN 0027-8424. doi: 10.1073/pnas.1213613110.

A. U. Tamuri, M. dos Reis, and R. A. Goldstein. Estimating the distribution of selection coefficients from phylogenetic data using sitewise mutation-selection models. *Genetics*, 190(3):1101–1115, mar 2012. ISSN 0016-6731. doi: 10.1534/genetics.111.136432.

UniProt Consortium. UniProt: a hub for protein information. *Nucleic Acids Research*, 43(Database issue):D204–12, jan 2015. ISSN 1362-4962. doi: 10.1093/nar/gku989.

A. I. Vatsiou, E. Bazin, and O. E. Gaggiotti. Detection of selective sweeps in structured populations: a comparison of recent methods. *Molecular Ecology*, 25(1):89–103, jan 2016. ISSN 09621083. doi: 10.1111/mec.13360.

D. M. Weinreich and L. Chao. Rapid evolutionary escape by large populations from local fitness peaks is likely in nature. *Evolution; International Journal of Organic Evolution*, 59(6):1175–1182, jun 2005. ISSN 0014-3820. doi: 10.1111/j.0014-3820.2005.tb01769.x.

M. T. Weirauch, A. Yang, M. Albu, A. G. Cote, A. Montenegro-Montero, P. Drewe, H. S. Najafabadi, S. A. Lambert, I. Mann, K. Cook, H. Zheng, A. Goity, H. van Bakel, J.-C. Lozano, M. Galli, M. G. Lewsey, E. Huang, T. Mukherjee, X. Chen, J. S. Reece-Hoyes, S. Govindarajan, G. Shaulsky, A. J. M. Walhout, F.-Y. Bouget, G. Ratsch, L. F. Larrondo, J. R. Ecker, and T. R. Hughes. Determination and inference of eukaryotic transcription factor sequence specificity. *Cell*, 158(6):1431–43, sep 2014. ISSN 1097-4172. doi: 10.1016/j.cell.2014.08.009.

D. B. Weissman, M. W. Feldman, and D. S. Fisher. The rate of fitness-valley crossing in sexual populations. *Genetics*, 186:1389–1410, 2010. doi: 10.1534/genetics.110.123240.

C. O. Wilke. The speed of adaptation in large asexual populations. *Genetics*, 167 (August):2045–2053, 2004. ISSN 0016-6731. doi: 10.1534/genetics.104.027136.

M. J. Wiser, N. Ribeck, and R. E. Lenski. Long-Term dynamics of adaptation in asexual populations. *Science*, 342(6164):1364–1367, dec 2013. ISSN 0036-8075. doi: 10.1126/science.1243357.

A. Wong and K. Seguin. Effects of genotype on rates of substitution during experimental evolution. *Evolution*, 69(7):1772–1785, 2015. ISSN 15585646. doi: 10.1111/evo.12700.

S. Wright. The roles of mutation, inbreeding, crossbreeding and selection in evolution, 1932. ISSN 0167-5273.

Y.-X. Zhang, K. Perry, V. A. Vinci, K. Powell, W. P. C. Stemmer, and S. B. del Cardayré. Genome shuffling leads to rapid phenotypic improvement in bacteria. *Nature*, 415(6872):644–646, feb 2002. ISSN 00280836. doi: 10.1038/415644a.

Figures

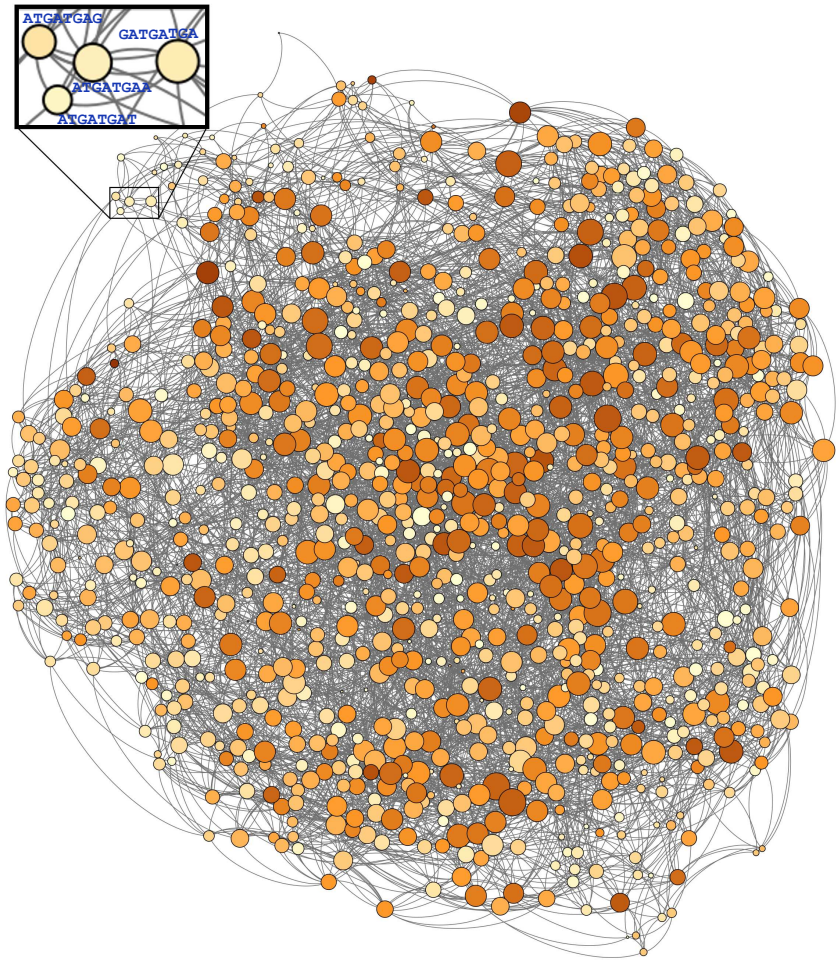

Fig. 1: **The adaptive landscape of the AZF2 transcription factor.** Each node corresponds to a DNA sequence. Two nodes are connected if they differ by a single point mutation or a single indel. Node color corresponds to the affinity of the sequence (Darker=Higher), and node size corresponds to the number of neighbors of the node (Bigger=More). The inset shows that two nodes are connected if they differ by a single mutation. Our display allows for overlapping nodes, so the actual number of nodes may be greater than the number of nodes that are visible.

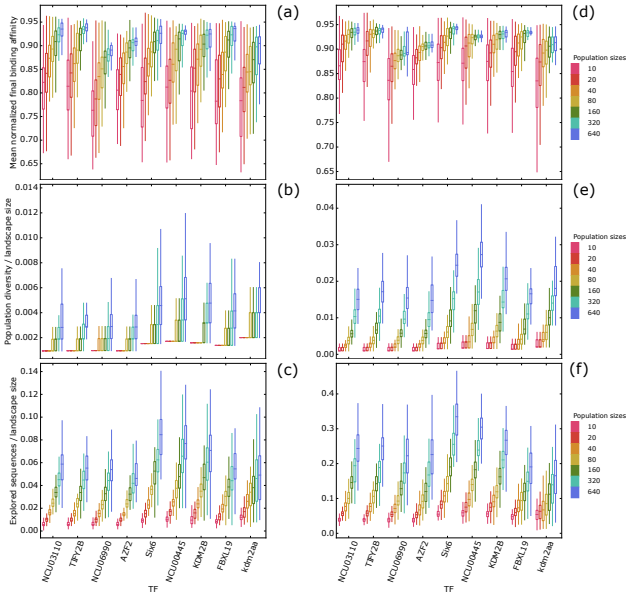

Fig. 2: **Mean final binding affinity, sequence exploration and diversity of populations at $\mu = 0.001$ and $\mu = 0.01$.** The figure shows **(a)** and **(d)** the mean population binding affinity at the end of the simulations for $\mu = 0.001$ and $\mu = 0.01$, respectively, **(b)** and **(e)** the population diversity at the end of the simulations, i.e. the number of unique sequences at generation 1,000, for $\mu = 0.001$ and $\mu = 0.01$, respectively, and **(c)** and **(f)** the total number of unique sequences visited by a population during 1,000 generations, for $\mu = 0.001$ and $\mu = 0.01$, respectively. Data in (a) and (d) are normalized by the maximum affinity value in each landscape, data in (b), (c), (e) and (f) are normalized by landscape size. Horizontal axes on all panels show different transcription factor affinity landscapes ordered from left to right in increasing order of ruggedness. We randomly selected a sequence of low binding affinity to initialize each simulation, and then simulated 1,000 generations of mutation and selection. We performed 100 replicate simulations for each population size at a fixed mutation rate of $\mu = 0.001$ and $\mu = 0.01$ per sequence per generation (see Methods). Each box encloses the second and third quartiles of data from 100 replicates, the center line corresponds to the median, and the whiskers depict the minimum and maximum values obtained from any replicate, excluding outliers.

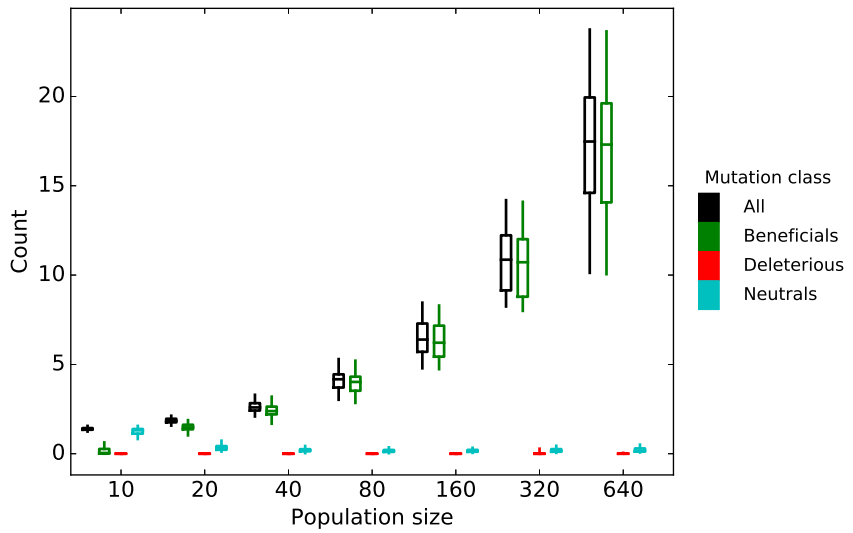

Fig. 3: **More beneficial mutations coexist in larger populations evolving on the AZF2 landscape at constant $\mu = 0.01$.** Boxplots summarize mean numbers of unique total, beneficial, deleterious, and neutral mutations that coexist per generation (color legend) for populations of different sizes (horizontal axis) evolved on the AZF2 landscape. When more than one beneficial mutation is present at the same time in a population, those mutations compete for fixation (clonal interference), resulting in longer fixation time for the mutation that finally fixes in the population. We determined the effect of each mutation compared to the ancestral sequence starting the population simulation. Effects smaller than $1/N$ are neutral. Each box encloses the second and third quartiles of data from 100 replicates, the center line corresponds to the median, and the whiskers depict the minimum and maximum values obtained from any replicate, excluding outliers. Population evolution was simulated in the same way as explained in the caption of Figure 2, except that $\mu = 0.01$.

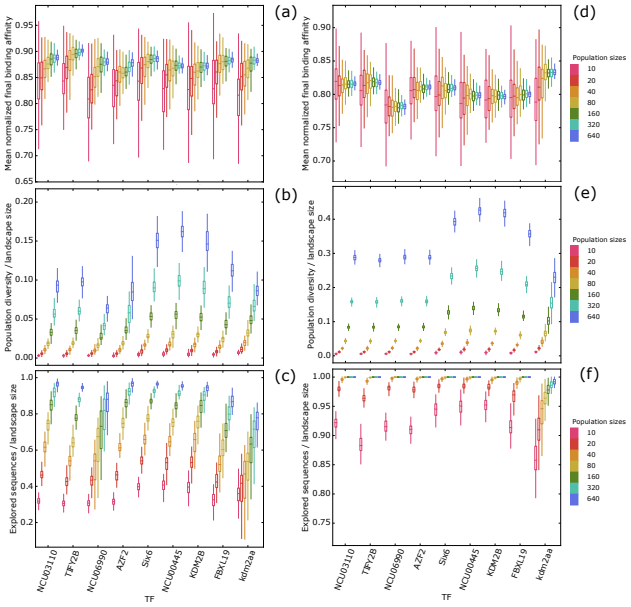

Fig. 4: **Mean final binding affinity, sequence exploration and diversity of populations at $\mu = 0.1$ and $\mu = 1$.** The figure shows **(a)** and **(d)** the mean population binding affinity at the end of the simulations for $\mu = 0.1$ and $\mu = 1$, respectively, **(b)** and **(e)** the population diversity at the end of the simulations, i.e. the number of unique sequences at generation 1,000, for $\mu = 0.1$ and $\mu = 1$, respectively, and **(c)** and **(f)** the total number of unique sequences visited by a population during 1,000 generations, for $\mu = 0.1$ and $\mu = 1$, respectively. Data in (a) and (d) are normalized by the maximum affinity value in each landscape, data in (b), (c), (e) and (f) are normalized by landscape size. Horizontal axes on all panels show different transcription factor affinity landscapes ordered from left to right in increasing order of ruggedness. Each box encloses the second and third quartiles of data from 100 replicates, the center line corresponds to the median, and the whiskers depict the minimum and maximum values obtained from any replicate, excluding outliers. Population evolution was simulated in the same way as explained in the caption of Figure 2, except that $\mu = 0.1$ and $\mu = 1$.

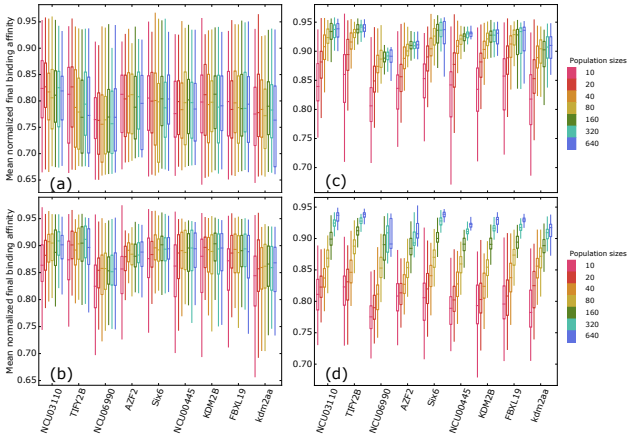

Fig. 5: **Mean population binding affinity at the end of the simulations at constant $N\mu$.** We randomly selected a sequence of low binding affinity to initialize each simulation, and then simulated 1,000 generations of mutation and selection. We performed 100 replicate simulations for each population size at a fixed population mutation rate of **(a)** $N\mu = 0.01$, **(b)** $N\mu = 0.1$, **(c)** $N\mu = 1$, and **(d)** $N\mu = 10$ per sequence per generation (see Methods). Each box encloses the second and third quartiles of data from 100 replicates, the center line corresponds to the median, and the whiskers depict the minimum and maximum values obtained from any replicate, excluding outliers. Data are normalized by the maximum binding affinity in the landscape.

Tables

Table 1: Landscapes in our study. Each column describes the following information: 'TF name': name of the transcription factor to which the sequences bind; 'Species': the species in which the transcription factor occurs; 'Number of components': number of connected components within each network, i.e., components in which sequences are accessible from one another through a path of one or more edges; 'Network size': total number of sequences in landscape; 'Size of the dominant genotype network': number of sequences in the largest connected component; 'Number of peaks': number of peaks in the landscape (see Methods); 'Study': the study from which data were retrieved for constructing the landscape.

TF name	**Species**	**Number of components**	**Network size**	**Size of the dominant genotype network**	**Number of peaks**	**Study**
NCU03110	*Neurospora crassa*	1	1,064	1,064	1	(Weirauch et al., 2014)
TIFY2B	*Arabidopsis thaliana*	1	1,050	1,050	1	(Weirauch et al., 2014)
NCU06990	*Neurospora crassa*	1	1,038	1,038	2	(Weirauch et al., 2014)
AZF2	*Arabidopsis thaliana*	1	1,051	1,051	3	(Weirauch et al., 2014)
Six6	*Mus musculus*	3	658	656	6	(Badis et al., 2009b)
NCU00445	*Neurospora crassa*	4	589	586	7	(Weirauch et al., 2014)
KDM2B	*Homo sapiens*	6	634	629	9	(Weirauch et al., 2014)
FBXL19	*Tetraodon nigroviridis*	7	730	724	13	(Weirauch et al., 2014)
kdm2aa	*Danio rerio*	13	513	499	36	(Weirauch et al., 2014)

Supplementary figures

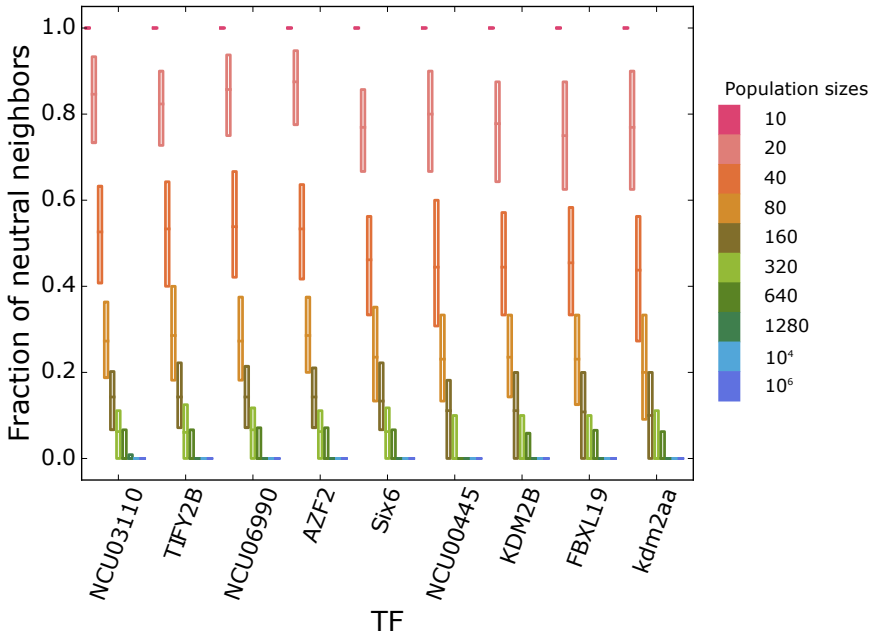

Fig. S1: **Fraction of neutral single-mutation neighbors.** For each of the nine landscapes we selected all sequences in the landscape and determined the fraction of neighbors with a binding affinity difference smaller than $1/N$ for a range of population sizes (legend). In these boxplots, each box encloses the second and third quartile of the fraction of neutral neighbors among all sequences. The center line corresponds to the median. As expected, the fraction of neutral neighbors decreases with increasing population size.

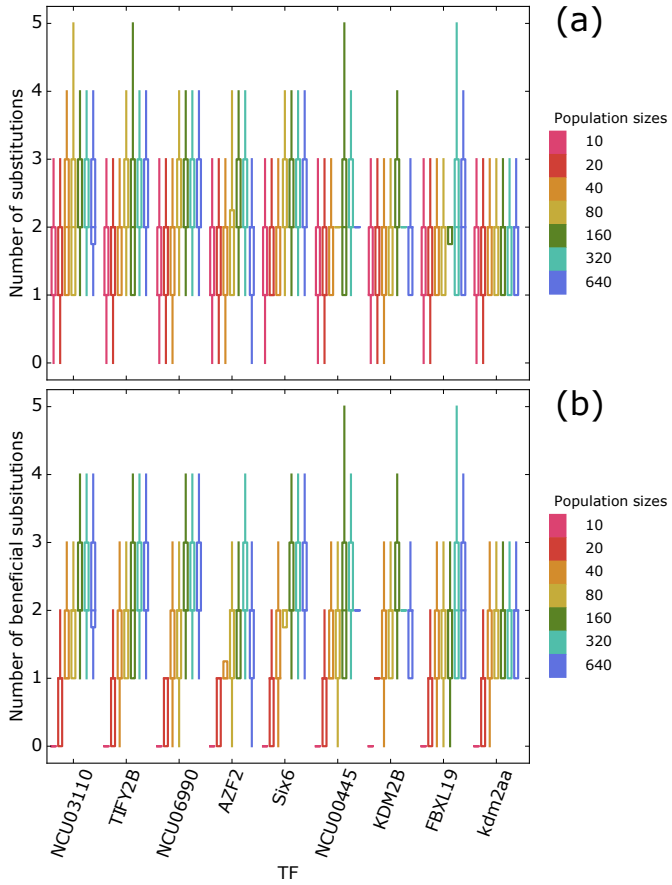

Fig. S2: **Numbers of total and beneficial substitutions at $\mu = 0.001$.** The figure shows the number of **(a)** all substitutions, and **(b)** beneficial substitutions in a population, for different population sizes (color legend) and different landscapes (horizontal axis). We defined a substitution as beneficial if the sequence had a fitness increase of more than $1/N$ compared to the sequence without the mutation. Each box encloses the second and third quartiles of data from 100 replicates, the center line corresponds to the median, and the whiskers depict the minimum and maximum values obtained from any replicate, excluding outliers. Population evolution was simulated in the same way as explained in the caption of Figure 2.

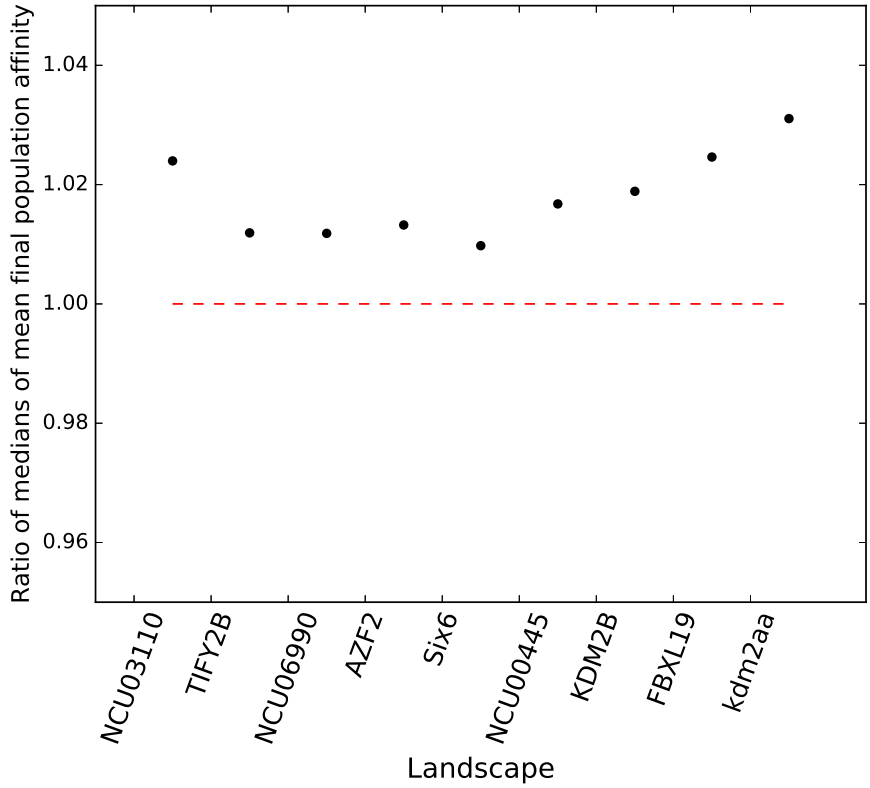

Fig. S3: **How mean population affinity changes between $N = 640$ and $N = 160$, at two different mutation rates ($\mu = 0.001$ and $\mu = 0.01$).** We first divided the median of mean final population affinities for all 100 simulation replicates of $N = 640$ to that of $N = 160$ when $\mu = 0.001$. We calculated the same ratios for populations evolved at $\mu = 0.01$. We finally divided the ratios at $\mu = 0.001$ to those at $\mu = 0.01$ and plotted them as circles in this figure. The circles above 1 indicate that the difference between mean final affinity of population at $N = 640$ to $N = 160$ is larger at the smaller mutation rate of $\mu = 0.001$.

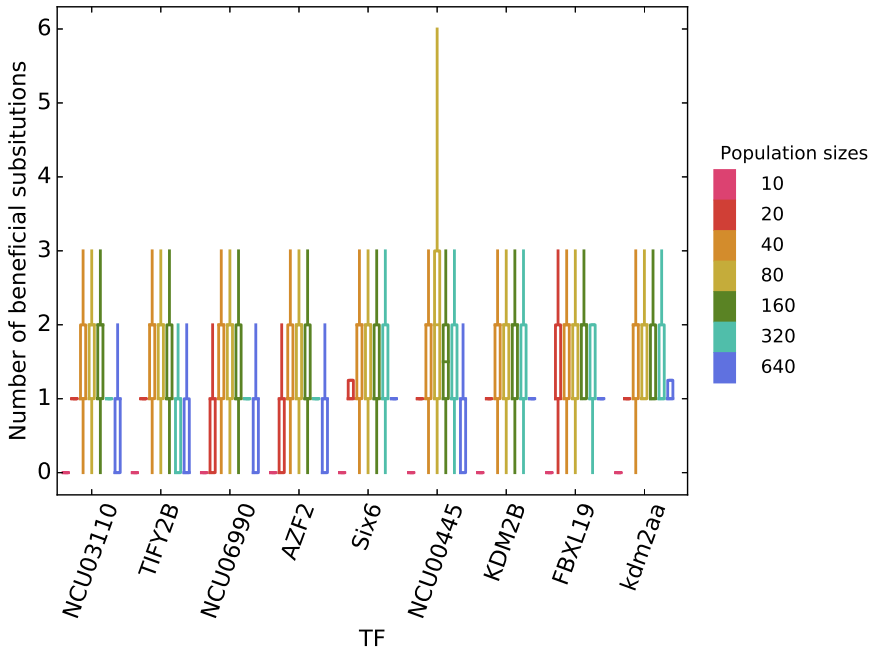

Fig. S4: **Number of beneficial substitutions in all simulations at constant $\mu = 0.01$.** Each boxplot summarizes the number of beneficial substitutions in 100 simulation replicates for different landscapes (horizontal axis) and population sizes (color legend). Each box encloses the second and third quartiles of data from 100 replicates, the center line corresponds to the median, and the whiskers depict the minimum and maximum values obtained from any replicate, excluding outliers. Population evolution was simulated in the same way as explained in the caption of Figure 2, except that $\mu = 0.01$.

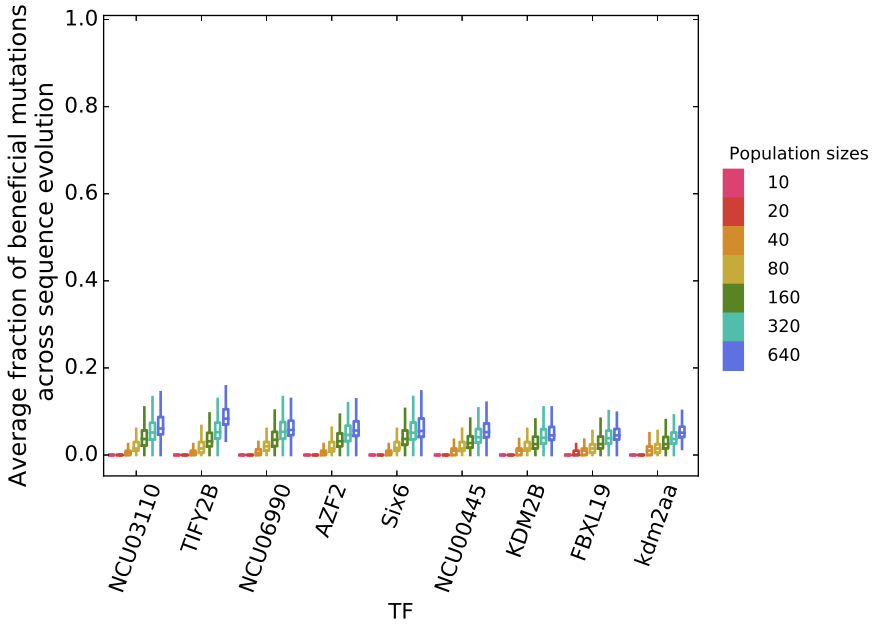

Fig. S5: **Fraction of beneficial mutations at constant $\mu = 0.01$.** Each boxplot summarizes the fraction of beneficial mutations in 100 simulation replicates for different landscapes (horizontal axis) and population sizes (color legend). Each box encloses the second and third quartiles of data from 100 replicates, the center line corresponds to the median, and the whiskers depict the minimum and maximum values obtained from any replicate, excluding outliers. Population evolution was simulated in the same way as explained in the caption of Figure 2, except that $\mu = 0.01$.

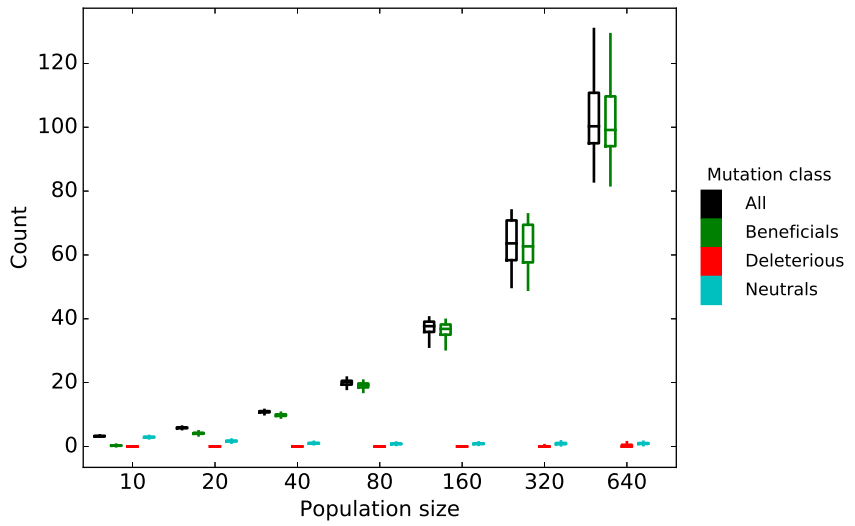

Fig. S6: **More beneficial mutations coexist in larger populations evolving on the AZF2 landscape at constant $\mu = 0.1$.** Boxplots summarize mean numbers of unique total, beneficial, deleterious, and neutral mutations that coexist per generation (color legend) for populations of different sizes (horizontal axis) evolved on the AZF2 landscape. When more than one beneficial mutation is present at the same time in a population, those mutations compete for fixation (clonal interference), resulting in longer fixation time for the mutation that finally fixes in the population. We determined the effect of each mutation compared to the ancestral sequence starting the population simulation. Effects smaller than $1/N$ are neutral. Each box encloses the second and third quartiles of data from 100 replicates, the center line corresponds to the median, and the whiskers depict the minimum and maximum values obtained from any replicate, excluding outliers. Population evolution was simulated in the same way as explained in the caption of Figure 2, except that $\mu = 0.1$.

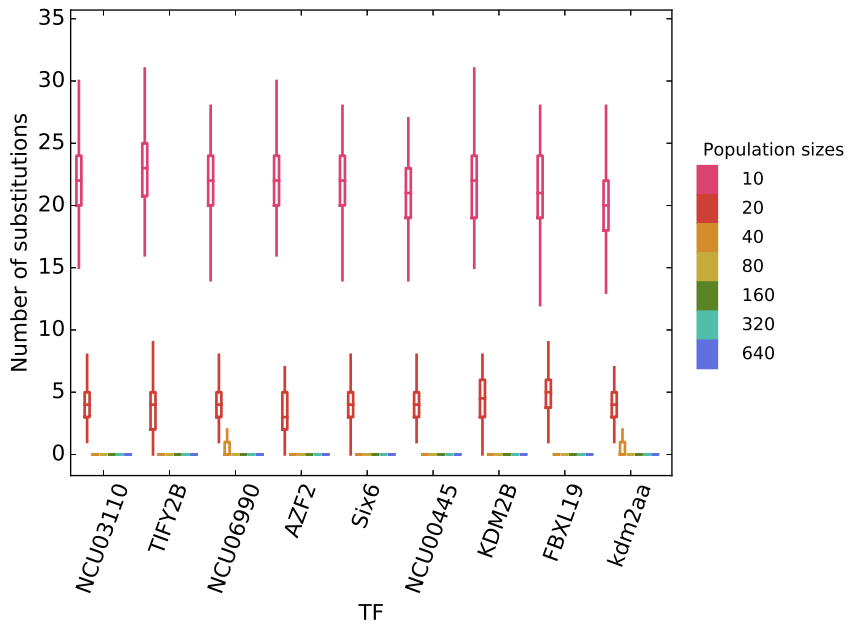

Fig. S7: **Numbers of all substitutions at $\mu = 0.1$.** The figure shows the number of substitutions in a population for different population sizes (color legend) and different landscapes (horizontal axis). Each box encloses the second and third quartiles of data from 100 replicates, the center line corresponds to the median, and the whiskers depict the minimum and maximum values obtained from any replicate, excluding outliers. Population evolution was simulated in the same way as explained in the caption of Figure 2, except that $\mu = 0.1$.

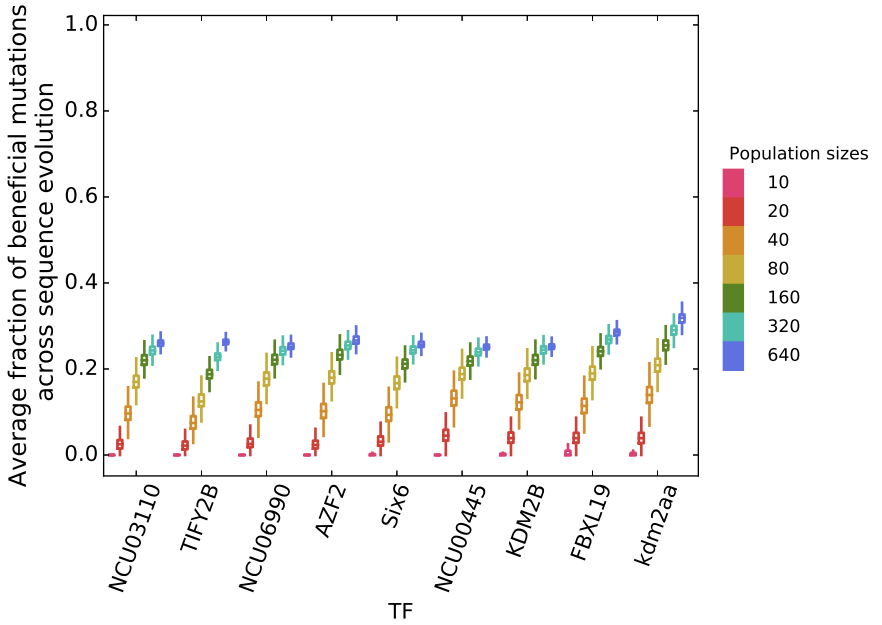

Fig. S8: **Fraction of beneficial mutations at constant $\mu = 0.1$.** Each boxplot summarizes the fraction of beneficial mutations in 100 simulation replicates for different landscapes (horizontal axis) and population sizes (color legend). Each box encloses the second and third quartiles of data from 100 replicates, the center line corresponds to the median, and the whiskers depict the minimum and maximum values obtained from any replicate, excluding outliers. Population evolution was simulated in the same way as explained in the caption of Figure 2, except that $\mu = 0.1$.

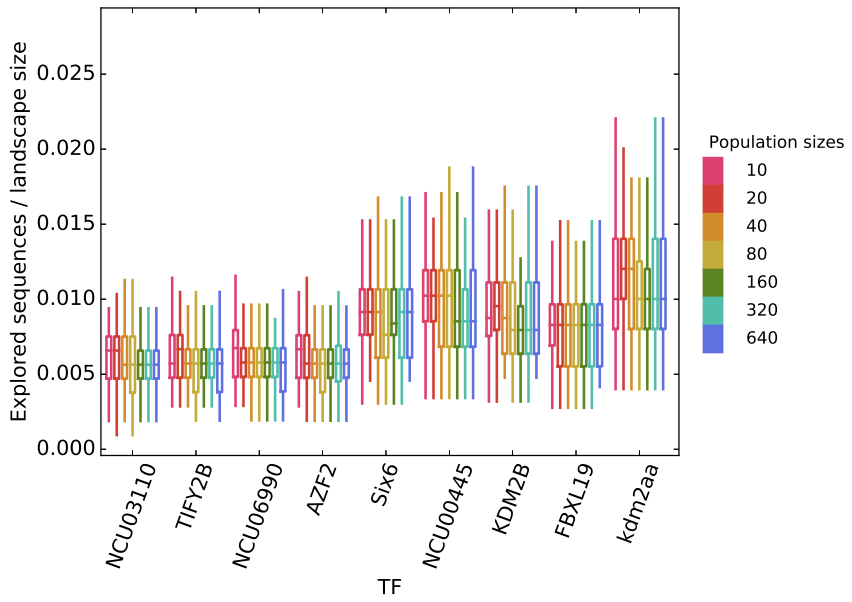

Fig. S9: **Number of explored sequences across generations at constant** $N\mu = 0.01$**.** The figure shows the total number of unique sequences visited by a population during 1,000 generations of simulated evolution for different population sizes (color legend), normalized by the size of each landscape (horizontal axis). Each box encloses the second and third quartiles of data from 100 replicates, the center line corresponds to the median, and the whiskers depict the minimum and maximum values obtained from any replicate, excluding outliers. Population evolution was simulated in the same way as explained in the caption of Figure 5a.

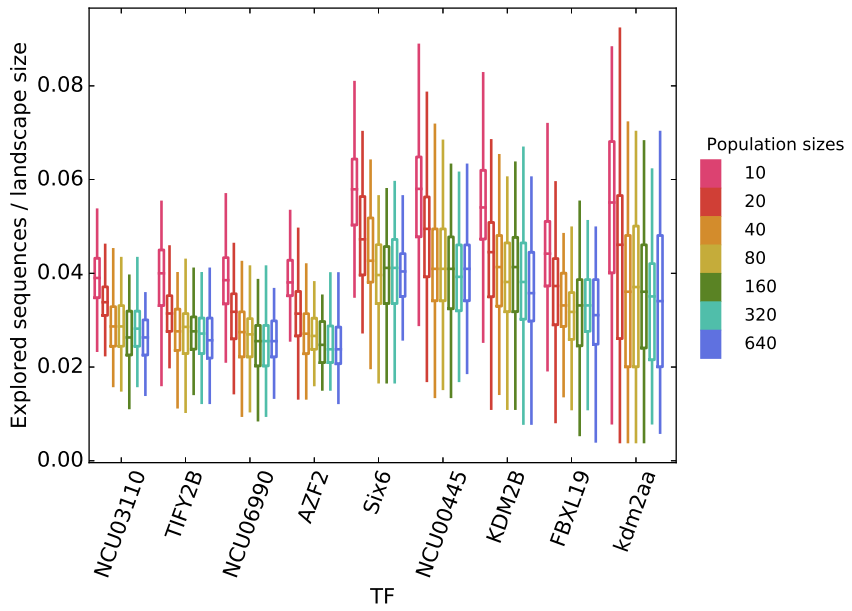

Fig. S10: **Number of explored sequences across generations at constant $N\mu = 0.1$.** The figure shows the total number of unique sequences visited by a population during 1,000 generations of simulated evolution for different population sizes (color legend), normalized by the size of each landscape (horizontal axis). Each box encloses the second and third quartiles of data from 100 replicates, the center line corresponds to the median, and the whiskers depict the minimum and maximum values obtained from any replicate, excluding outliers. Population evolution was simulated in the same way as explained in the caption of Figure 5a, except that $N\mu = 0.1$.

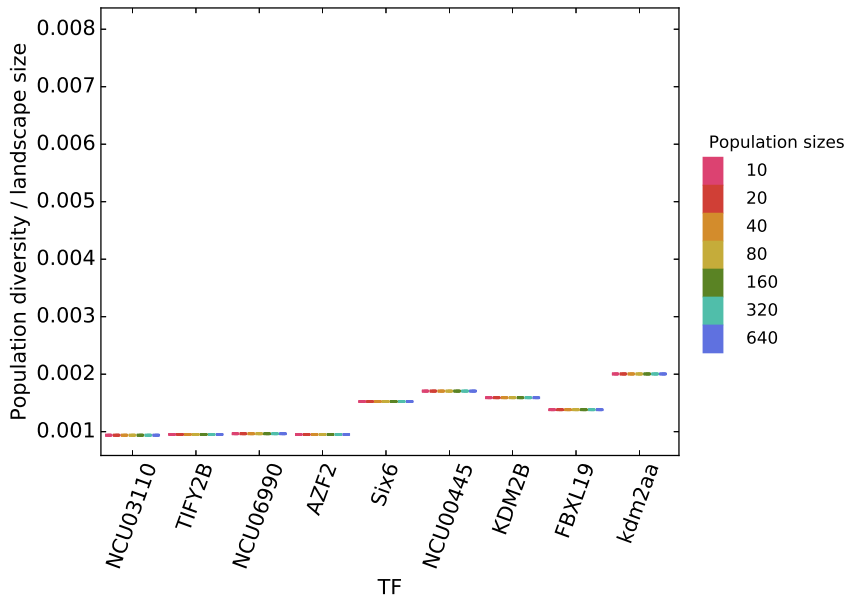

Fig. S11: **Population diversity at the end of simulations at constant** $N\mu = 0.01$**.** The figure shows the number of unique sequences at generation 1,000 of simulated evolution for different population sizes (color legend), normalized by the size of each landscape (horizontal axis). Each box encloses the second and third quartiles of data from 100 replicates, which are smaller than the line width in this plot The center line corresponds to the median, and the whiskers depict the minimum and maximum values obtained from any replicate, excluding outliers. Population evolution was simulated in the same way as explained in the caption of Figure 5a.

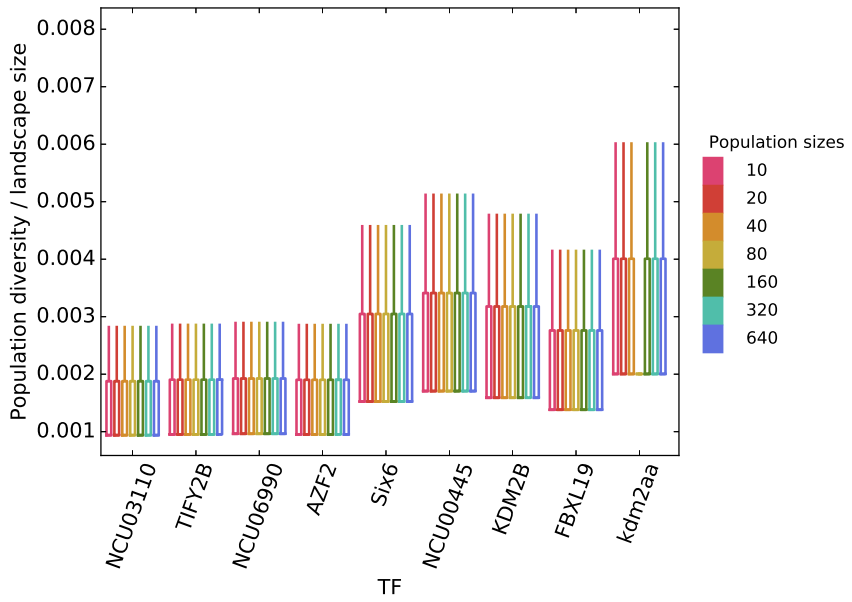

Fig. S12: **Population diversity at the end of simulations at constant** $N\mu = 0.1$**.** The figure shows the number of unique sequences at generation 1,000 of simulated evolution for different population sizes (color legend), normalized by the size of each landscape (horizontal axis). Each box encloses the second and third quartiles of data from 100 replicates. The center line corresponds to the median, and the whiskers depict the minimum and maximum values obtained from any replicate, excluding outliers. Population evolution was simulated in the same way as explained in the caption of Figure 5a, except that $N\mu = 0.1$.

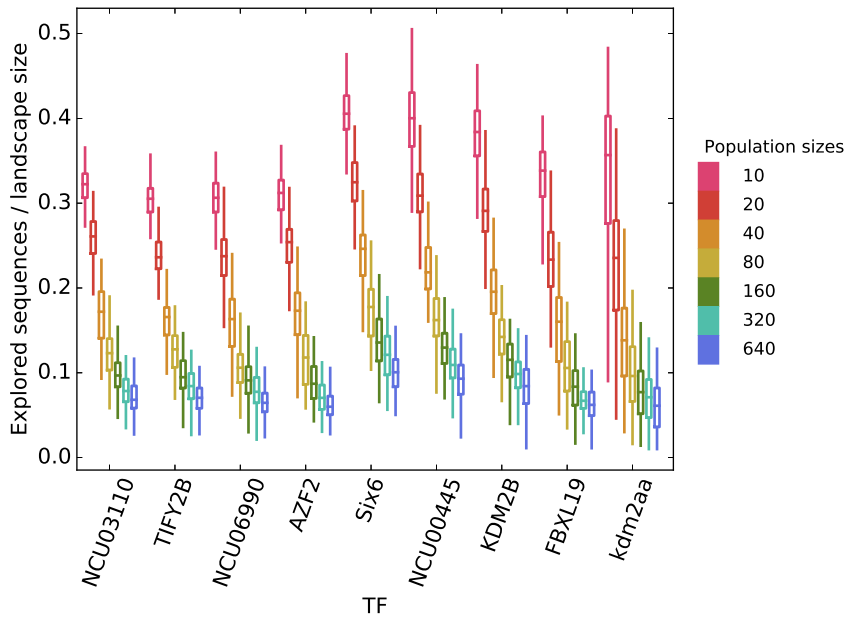

Fig. S13: **Number of explored sequences across generations at constant $N\mu = 1$.** The figure shows the total number of unique sequences visited by a population during 1,000 generations of simulated evolution for different population sizes (color legend), normalized by the size of each landscape (horizontal axis). Each box encloses the second and third quartiles of data from 100 replicates, the center line corresponds to the median, and the whiskers depict the minimum and maximum values obtained from any replicate, excluding outliers. Population evolution was simulated in the same way as explained in the caption of Figure 5a, except that $N\mu = 1$.

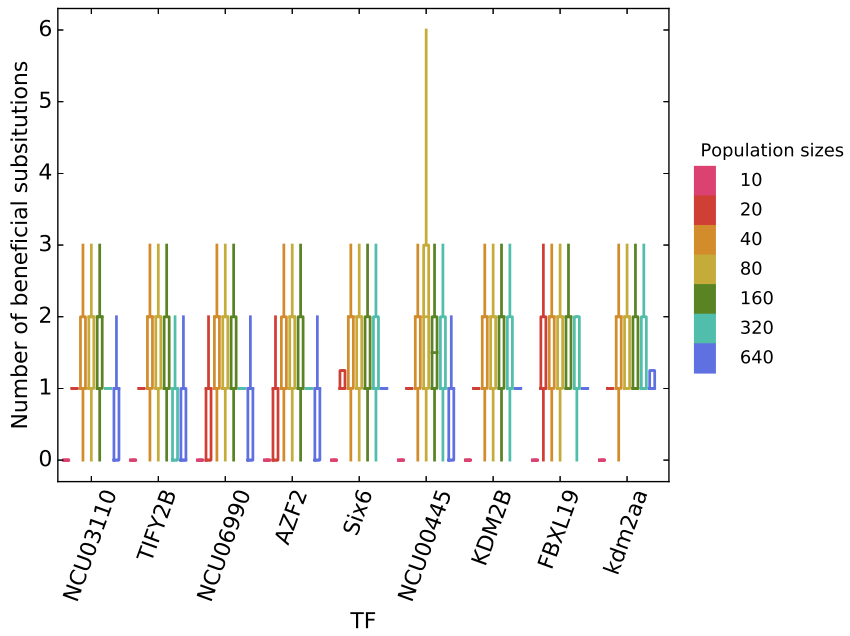

Fig. S14: **Number of explored sequences across generations at constant $N\mu = 10$.** The figure shows the total number of unique sequences visited by a population during 1,000 generations of simulated evolution for different population sizes (color legend), normalized by the size of each landscape (horizontal axis). Each box encloses the second and third quartiles of data from 100 replicates, the center line corresponds to the median, and the whiskers depict the minimum and maximum values obtained from any replicate, excluding outliers. Population evolution was simulated in the same way as explained in the caption of Figure 5a, except that $N\mu = 10$.

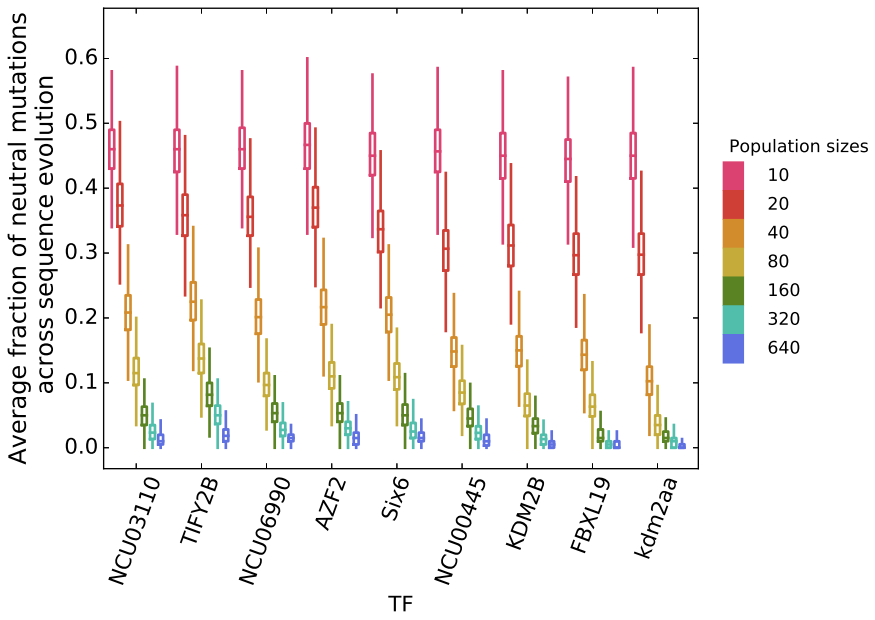

Fig. S15: **Fraction of neutral mutations at constant** $N\mu = 1$**.** Each boxplot summarizes the fraction of neutral mutations in 100 simulation replicates for different landscapes (horizontal axis) and population sizes (color legend). Each box encloses the second and third quartiles of data from 100 replicates, the center line corresponds to the median, and the whiskers depict the minimum and maximum values obtained from any replicate, excluding outliers. Population evolution was simulated in the same way as explained in the caption of Figure 5a, except that $N\mu = 1$.

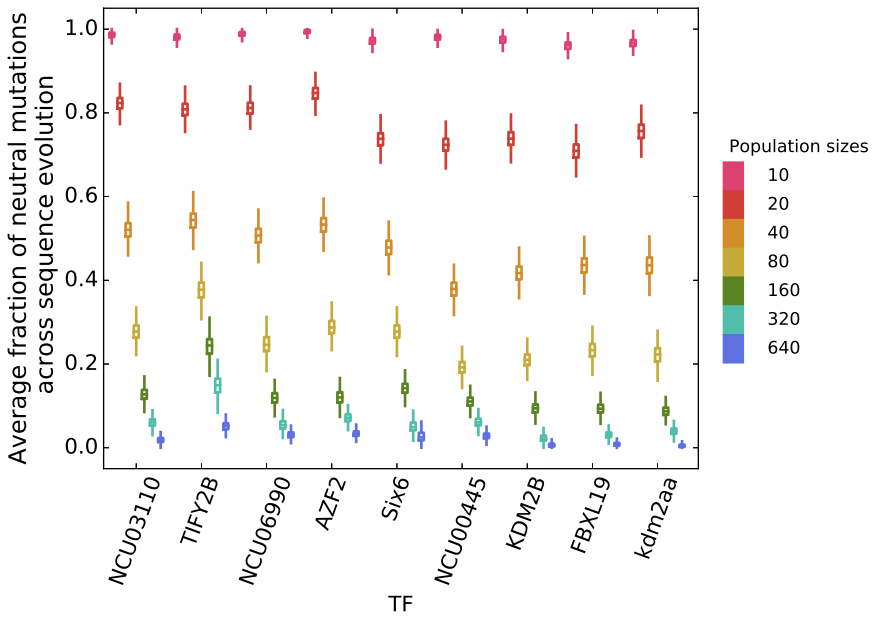

Fig. S16: **Fraction of neutral mutations at constant** $N\mu = 10$**.** Each boxplot summarizes the fraction of neutral mutations in 100 simulation replicates for different landscapes (horizontal axis) and population sizes (color legend). Each box encloses the second and third quartiles of data from 100 replicates, the center line corresponds to the median, and the whiskers depict the minimum and maximum values obtained from any replicate, excluding outliers. Population evolution was simulated in the same way as explained in the caption of Figure 5a, except that $N\mu = 10$.

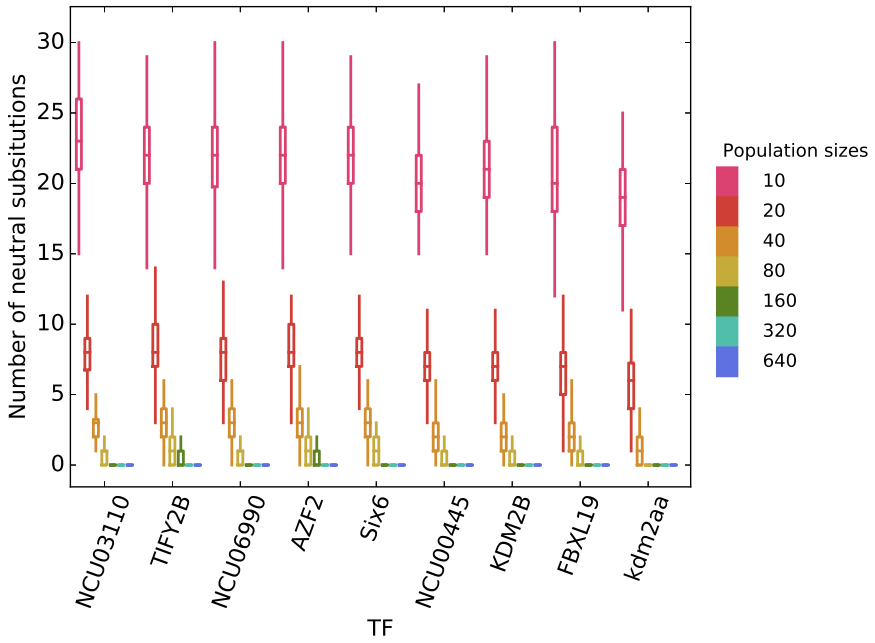

Fig. S17: **Number of neutral substitutions at constant $N\mu = 1$.** Each boxplot summarizes the number of neutral substitutions in 100 simulation replicates for different landscapes (horizontal axis) and population sizes (color legend). Each box encloses the second and third quartiles of data from 100 replicates, the center line corresponds to the median, and the whiskers depict the minimum and maximum values obtained from any replicate, excluding outliers. Population evolution was simulated in the same way as explained in the caption of Figure 5a, except that $N\mu = 1$.

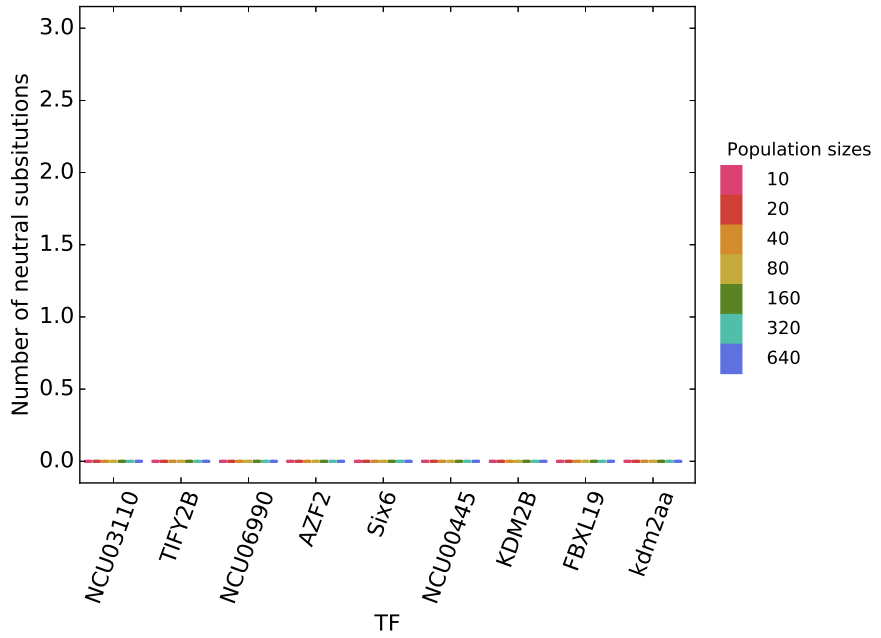

Fig. S18: **Number of neutral substitutions at constant $N\mu = 10$.** Each boxplot summarizes the number of neutral substitutions in 100 simulation replicates for different landscapes (horizontal axis) and population sizes (color legend). Each box encloses the second and third quartiles of data from 100 replicates, the center line corresponds to the median, and the whiskers depict the minimum and maximum values obtained from any replicate, excluding outliers. Population evolution was simulated in the same way as explained in the caption of Figure 5a, except that $N\mu = 10$.

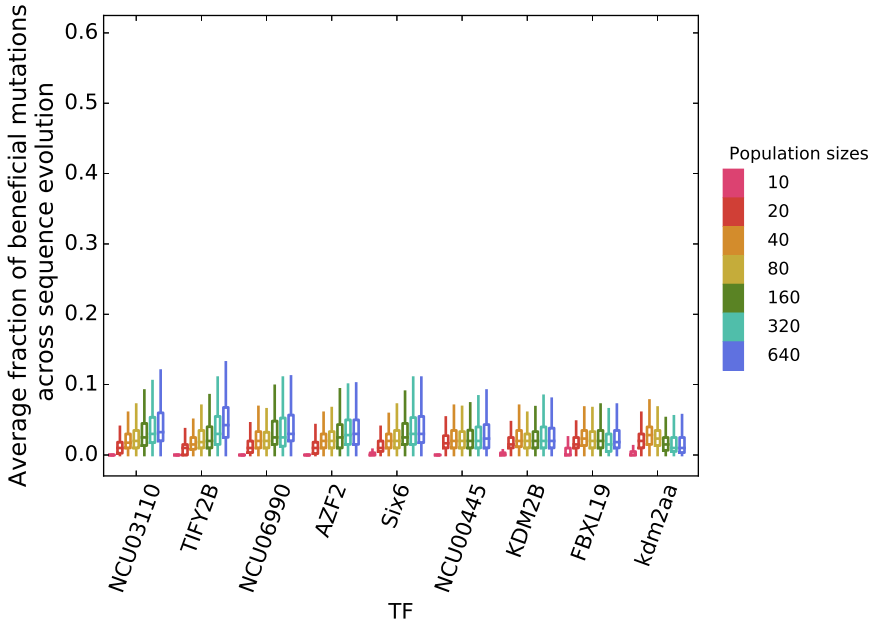

Fig. S19: **Fraction of beneficial mutations at constant $N\mu = 1$.** Each boxplot summarizes the fraction of beneficial mutations in 100 simulation replicates for different landscapes (horizontal axis) and population sizes (color legend). Each box encloses the second and third quartiles of data from 100 replicates, the center line corresponds to the median, and the whiskers depict the minimum and maximum values obtained from any replicate, excluding outliers. Population evolution was simulated in the same way as explained in the caption of Figure 5a, except that $N\mu = 1$.

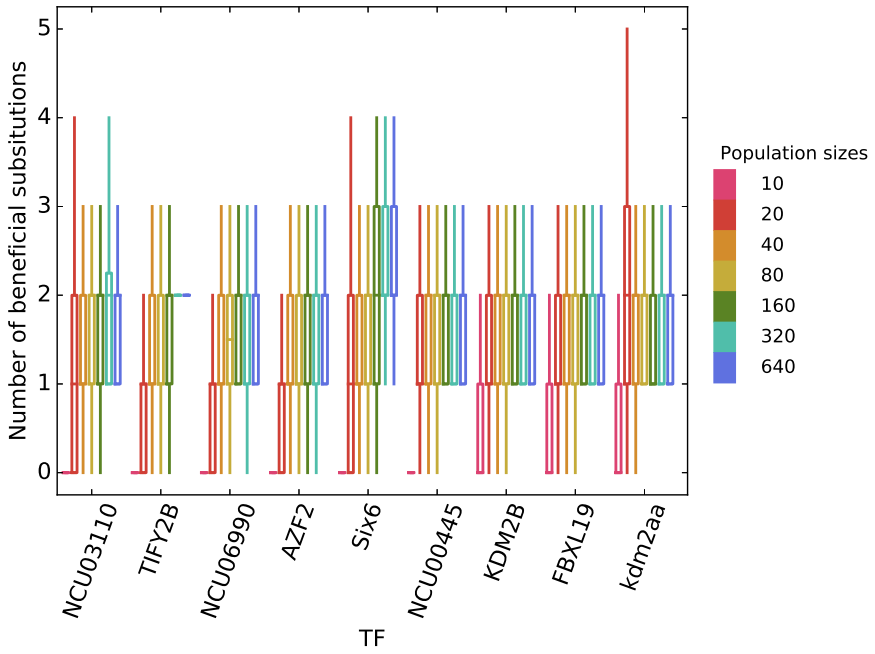

Fig. S20: **Fraction of beneficial substitutions at constant $N\mu = 1$.** Each boxplot summarizes the fraction of beneficial substitutions in 100 simulation replicates for different landscapes (horizontal axis) and population sizes (color legend). Each box encloses the second and third quartiles of data from 100 replicates, the center line corresponds to the median, and the whiskers depict the minimum and maximum values obtained from any replicate, excluding outliers. Population evolution was simulated in the same way as explained in the caption of Figure 5a, except that $N\mu = 1$.

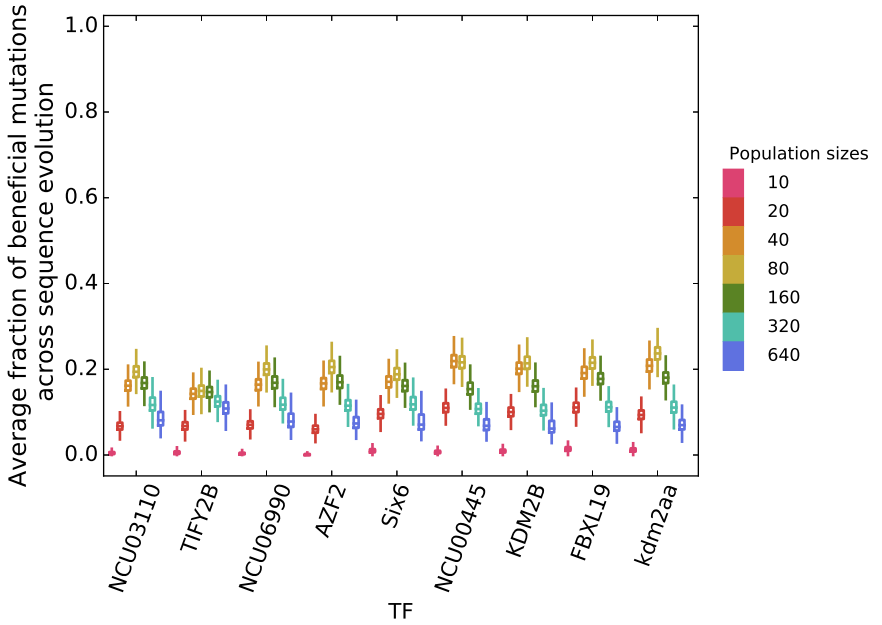

Fig. S21: **Fraction of beneficial mutations at constant $N\mu = 10$.** Each boxplot summarizes the fraction of beneficial mutations in 100 simulation replicates for different landscapes (horizontal axis) and population sizes (color legend). Each box encloses the second and third quartiles of data from 100 replicates, the center line corresponds to the median, and the whiskers depict the minimum and maximum values obtained from any replicate, excluding outliers. Population evolution was simulated in the same way as explained in the caption of Figure 5a, except that $N\mu = 10$. The likely reason why peaks occur at intermediate population sizes is that smaller populations experience fewer beneficial mutations, because selection is less efficient for them, and larger populations, having reached higher levels in the landscape, have a different distribution of fitness effects with fewer beneficial mutations. Therefore, populations at intermediate sizes experience the most beneficial mutations.

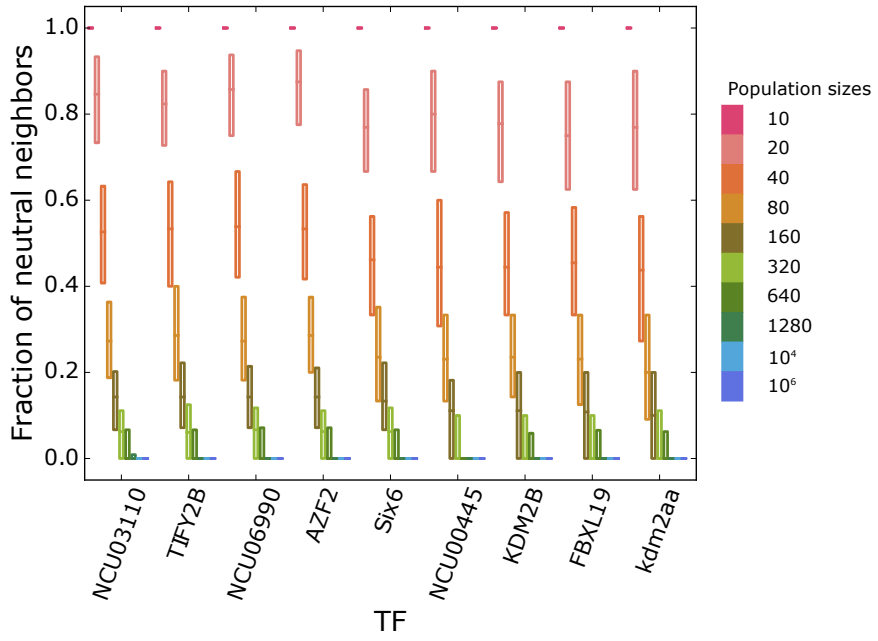

Fig. S22: **Fraction of beneficial substitutions at constant** $N\mu = 10$**.** Each boxplot summarizes the fraction of beneficial substitutions in 100 simulation replicates for different landscapes (horizontal axis) and population sizes (color legend). Each box encloses the second and third quartiles of data from 100 replicates, the center line corresponds to the median, and the whiskers depict the minimum and maximum values obtained from any replicate, excluding outliers. Population evolution was simulated in the same way as explained in the caption of Figure 5a, except that $N\mu = 10$.

Table S1: Correlations between number of peaks in each of 957 landscapes with 100 or more sequences (Aguilar-Rodríguez et al., 2017) and mean affinity of populations at generation 1,000. Each row of the table represents the correlation between the mean final affinity of 100 simulation replicates for each of the landscapes at a given mutation rate, and the number of peaks in those landscapes. We normalized the mean final affinity of each population by the maximum binding affinity in the landscape.

Population size	**Mutation rate**	**Spearman's ρ**	**p-value**
10	0.001	-0.331	0
20	0.001	-0.356	0
40	0.001	-0.249	0
80	0.001	-0.155	0
160	0.001	-0.285	0
320	0.001	-0.205	0
640	0.001	-0.382	0
10	0.01	-0.379	0
20	0.01	-0.389	0
40	0.01	-0.324	0
80	0.01	-0.240	0
160	0.01	-0.353	0
320	0.01	-0.284	0
640	0.01	-0.394	0
10	0.1	-0.407	0
20	0.1	-0.438	0
40	0.1	-0.330	0
80	0.1	-0.240	0
160	0.1	-0.365	0
320	0.1	-0.283	0
640	0.1	-0.459	0
10	1	-0.433	0
20	1	-0.450	0
40	1	-0.365	0
80	1	-0.257	0
160	1	-0.407	0
320	1	-0.309	0
640	1	-0.460	0

Supplementary tables

Table S2: Correlations between size of the global peak in each of 957 landscapes 100 or more sequences (Aguilar-Rodríguez et al., 2017) and mean affinity of populations at generation 1,000. Each row of the table represents the correlation between the mean final affinity of 100 simulation replicates for each of the landscapes at a given mutation rate, and the size of the global peak in those landscapes. We normalized the mean final affinity of each population by the maximum binding affinity in the landscape.

Population size	**Mutation rate**	**Spearman's ρ**	**p-value**
10	0.001	0.356	0
20	0.001	0.395	0
40	0.001	0.272	0
80	0.001	0.166	0
160	0.001	0.311	0
320	0.001	0.225	0
640	0.001	0.434	0
10	0.01	0.453	0
20	0.01	0.491	0
40	0.01	0.345	0
80	0.01	0.265	0
160	0.01	0.400	0
320	0.01	0.295	0
640	0.01	0.514	0
10	0.1	0.537	0
20	0.1	0.583	0
40	0.1	0.410	0
80	0.1	0.292	0
160	0.1	0.470	0
320	0.1	0.345	0
640	0.1	0.619	0
10	1	0.568	0
20	1	0.594	0
40	1	0.472	0
80	1	0.326	0
160	1	0.531	0
320	1	0.402	0
640	1	0.606	0

Table S3: Biological functions of transcription factors whose landscapes we have used in this study. We used UniProt (UniProt Consortium, 2015) for finding the functions of the factors, and CIS-BP database (Weirauch et al., 2014) for finding the DNA binding domain classes.

ID	Full name	Function	DNA binding domain class
NCU03110	Uncharacterized		Zinc cluster
TIFY2B	GATA transcription factor 24	A transcriptional activator that binds to gene promoters.	GATA
NCU06990	Uncharacterized		Zinc cluster
AZF2	Zinc finger protein AZF2	A transcriptional repressor that prevents plant growth.	C2H2 ZF
Six6	Homeobox protein SIX6	Probably affects eye development.	
NCU00445	Uncharacterized		Zinc cluster
KDM2B	Lysine-specific demethylase 2B	Prevents cell growth and proliferation by repressing the transcription of ribosomal RNA genes.	CxxC
FBXL19	F-box/LRR-repeat protein 19	Part of the SCF (SKP1-CUL1-F-box protein)-type E3 ubiquitin ligase complex.	CxxC
kdm2aa	Uncharacterized		CxxC

Table S4: Correlation between the mean final binding affinity of all simulated populations, normalized by the maximum affinity in each landscape, and the number of unique sequences at generation 1,000 at constant $\mu = 0.01$. P-values are corrected for multiple testing using FDR.

TF	**Spearman's ρ**	**p-value**
NCU03110	0.42	9.56E-31
TIFY2B	0.45	1.14E-35
NCU06990	0.39	4.25E-27
AZF2	0.37	1.80E-24
Six6	0.49	1.38E-42
NCU00445	0.27	4.97E-13
KDM2B	0.46	1.22E-37
FBXL19	0.33	1.77E-19
kdm2aa	0.35	8.27E-22

Table S5: Correlation between the mean final binding affinity of all simulated populations, normalized by the maximum affinity in each landscape, and the number of explored sequences at constant $\mu = 0.01$. P-values are corrected for multiple testing using FDR.

TF	**Spearman's ρ**	**p-value**
NCU03110	0.51	1.71E-46
TIFY2B	0.59	5.33E-67
NCU06990	0.43	3.27E-32
AZF2	0.43	1.33E-32
Six6	0.65	7.76E-83
NCU00445	0.44	6.11E-35
KDM2B	0.62	3.13E-76
FBXL19	0.48	4.58E-42
kdm2aa	0.61	5.04E-71

Table S6: Correlation between the mean final binding affinity of all simulated populations, normalized by the maximum affinity in each landscape, and the number of beneficial mutations at constant $\mu = 0.01$. P-values are corrected for multiple testing using FDR.

TF	**Spearman's ρ**	**p-value**
NCU03110	0.56	3.75E-57
TIFY2B	0.53	1.09E-50
NCU06990	0.50	8.72E-45
AZF2	0.53	2.39E-51
Six6	0.58	1.52E-64
NCU00445	0.44	7.23E-34
KDM2B	0.55	1.99E-56
FBXL19	0.48	3.92E-42
kdm2aa	0.44	4.48E-34

Table S7: Correlation between the mean final binding affinity of all simulated populations, normalized by the maximum affinity in each landscape, and the number of beneficial substitutions at constant $\mu = 0.1$. p-values are corrected for multiple testing using FDR.

TF	**Spearman's ρ**	**p-value**
NCU03110	0.43	3.17E-32
TIFY2B	0.53	1.86E-51
NCU06990	0.62	2.12E-74
AZF2	0.45	2.16E-36
Six6	0.39	5.06E-26
NCU00445	0.36	8.74E-23
KDM2B	0.36	4.78E-23
FBXL19	0.32	7.02E-18
kdm2aa	0.54	4.86E-54

Table S8: Delta (Δ) values used in our simulations as a measure of noise in measured affinity E-scores, taken from (Aguilar-Rodríguez et al., 2017).

TF name	**Delta**
NCU03110	0.024419
TIFY2B	0.024981
NCU06990	0.028733
AZF2	0.022419
Six6	0.024746
NCU00445	0.031016
KDM2B	0.028908
FBXL19	0.028274
kdm2aa	0.028421